Origin and evolutionary trajectories of brown algal sex chromosomes

Authors: Josué Barrera-Redondo[1#], Agnieszka P. Lipinska[1,4#], Pengfei Liu[1], Erica Dinatale[1], Guillaume Cossard[1], Kenny Bogaert[1], Masakazu Hoshino[1,2], Komlan Avia[3], Goncalo Leiria[1], Elena Avdievich[1], Daniel Liesner[1], Rémy Luthringer[1], Olivier Godfroy[4], Svenja Heesch[4], Zofia Nehr[4], Loraine Brillet-Guéguen[4], Akira F. Peters[5], Galice Hoarau[7], Gareth Pearson[6], Jean-Marc Aury[8], Patrick Wincker[8], France Denoeud[8,Φ], J Mark Cock[4,Φ], Fabian B. Haas[1,Φ], Susana M Coelho[1,Φ*]

[1]Department of Algal Development and Evolution, Max Planck Institute for Biology Tübingen, 72076 Tübingen, Germany, [2]Current address: Research Center for Inland Seas, Kobe University, Rokkodai 1-1, Nadaku, Kobe 657-8501, Japan; [3]INRAE, Université de Strasbourg, UMR SVQV, 68000 Colmar, France; [4]Station Biologique de Roscoff CNRS, Sorbonne Universite, France; [5]Bezhin Rosko, 29250 Santeg, France; [6]Universidade do Algarve, UALG · Centro de Ciências do Mar (CCMAR); [7]Faculty of Biosciences and Aquaculture, Nord University, 8026 Bodø, Norway; [8]Génomique Métabolique, Genoscope, Institut François Jacob, CEA, CNRS, Univ Evry, Université Paris-Saclay, Evry, 91057, France.

[#]Equal contribution

[Φ]senior authors

[*]Lead author: susana.coelho@tuebingen.mpg.de

Running title: Retracing the complex evolutionary history of sex chromosomes across brown seaweeds

HIGHLIGHTS

Sexes arose in brown algae due to ceased recombination of a male-determining gene-containing region

U/V sex chromosomes evolve via gene gain and act as 'cradles' of genomic novelty

Emergence of XX/XY chromosomes involved demotion of the V-master sex-determining gene

Introgression of female-specific genes into a male background allowed hermaphroditism to arise

SUMMARY

Sex chromosomes fall into three classes: XX/XY, ZW/ZZ and U/V systems. The rise, evolution and demise of U/V systems have remained enigmatic to date. Here, we analyze genomes spanning the entire brown algal phylogeny to decipher their sex-determination evolutionary history. The birth of U/V sex chromosomes evolved more than 250 million years ago, when a pivotal male-determinant located in a discrete region in proto-U and proto-V chromosomes ceased recombining. Over time, nested inversions led to step-wise expansions, accompanying increasing morphological complexity and sexual differentiation of brown seaweeds. Unlike XX/XY and ZW/ZZ, U/V evolve mainly by gene gain, showing minimal degeneration. They are structurally dynamic, and act as genomic 'cradles' fostering the birth of new genes. Our analyses show that hermaphroditism arose from ancestral males that acquired U-specific genes by ectopic recombination, and that in the transition from a U/V to an XX/XY system, V-specific genes moved down the genetic hierarchy of sex determination. Both events lead to the demise of U and V and erosion of their specific genomic characteristics. Taken together, our findings offer a comprehensive model of U/V sex chromosome evolution.

INTRODUCTION

Sexual reproduction ensures the generation of new genetic combinations in nearly all eukaryotic species. The core mechanisms of sexual reproduction (meiosis and syngamy) are conserved, yet the pathways that determine the male and female identities are remarkably labile across eukaryotes[1,2]. Genetic determination of sex is mediated by sex chromosomes, whose programmatic domain is a sex-determining region (SDR) that carries the sex-determining factor(s) and usually does not recombine in the heterogametic sex. The SDR can be as small as a single locus or as large as an entire chromosome[3]. Sex chromosomes originate from autosomes (*i.e.*, any chromosome that is not a sex chromosome) and have independently and repeatedly evolved in different lineages. They are subject to unique evolutionary forces, including sex-specific selection, asymmetrical sheltering of deleterious mutations, hemizygosity, and dosage compensation[3]. They also play prominent roles in evolutionary processes such as speciation and adaptation[4], and are thought to be associated with the evolution of anisogamy and with the regulation of key life cycle transitions[5].

Knowledge about the biology and evolution of sex chromosomes stems from a few well-studied model organisms, notably mammals, birds, fish and *Drosophila*[6]. While studies so far have primarily focused on diploid sex determination systems (the classical XX/XY or ZW/ZZ systems), haploid phase sex-determination systems (U/V systems) such as those of mosses and brown, red and green algae[7,8] remain largely unexplored. Although U/V, XX/XY and ZW/ZZ systems share several core features, there are important differences between them that have broad evolutionary and genomic implications[9]. Comparing the evolutionary trajectories of XX/XY, ZW/ZZ and U/V chromosomes, together with comparisons with species that lack sex chromosomes entirely, offer opportunities to assess the relative importance of the forces driving the evolution of each system. However, only a few U/V sex chromosomes have been sequenced to date, namely the U/V system of *Ceratodon*[10], a peat moss (*Sphagnum*)[11], *Marchantia*[12] and the U chromosome of *Syntrichia caninervis*[13], all belonging to the Archeaplastida (land plant) lineage. Consequently, we currently lack a broad-scale comparison across several U/V sex chromosome systems that would inform a reconstruction of their evolutionary history.

In this context, brown algae (Phaeophyceae) represent exceptional models for investigating the origins and evolution of sex chromosomes. They span a bewildering variety of reproductive systems, life cycles and sex chromosome systems in a single lineage[14]. The maintenance of this range of variability in a single group is unique among Eukaryotes, and clearly points to a complex evolutionary history of their underlying sex-determination systems.

Here, we exploit a range of brown algal species and outgroups with diverse types of sexual systems to study the origin, evolution and demise of the U/V sex chromosomes. We show that separate sexes arose in the brown seaweeds >250 million years ago (Mya), when a small region in the proto-U and proto-V chromosomes that encodes expression of a master male-sex determinant stopped recombining. This event was followed by lineage-specific and step-wise expansion of the sex-locus that accompanied both the increased morphological complexity and the degree of sexual dimorphism. Brown algal U/V sex chromosomes are structurally highly dynamic, except for the genes specifically involved in sex determination and differentiation, evolve primarily by gene gain and act as 'cradles' for genomic novelty. Emergence of a diploid XX/XY sex chromosome system from the ancestral U/V involved movement of master sex determining gene(s) down in the sex-determination

hierarchy. Finally, we show that repeated transitions from U/V to hermaphroditism occurred via introgression of female SDR genes into a male background, leading to the demise of the sex chromosomes. Our work, therefore, has allowed the reconstruction of the evolutionary history of U/V sex chromosomes and opens new avenues to the study of this ecologically relevant eukaryotic lineage.

RESULTS

Identification and characterization of brown algal sex chromosomes

Brown seaweed are eukaryotic organisms spanning a rich variety of morphologies, life cycles and sexual systems[8,14,15]. Using high-quality reference genomes (Denoeud et al, submitted), supplemented with genetic and HiC physical maps (see methods), we generated chromosome or near-chromosome level genome assemblies of nine representative brown algal species. Collectively, and together with the outgroup species *Schizocladia ischiensis*[16], these span the phylogenetic, morphological and reproductive diversity of brown seaweeds[15] (**Fig. 1A**). Overall, our analyses reveal that brown algae have a relatively stable karyotype (27-33 chromosomes) and a well conserved macrosynteny (*i.e.*, similar blocks of genes located in the same relative positions in the genome across species) (**Fig. 1A**).

Using comparative genomic approaches combined with experimental validation of sex-linkage using PCR (see methods) we identified the SDR on the sex chromosomes for each of the dioicous species (**Fig. 1A**). Consistent with dioicy being the ancestral state in the brown algal lineage[14], the synteny analysis demonstrated that all species with a U/V sexual system shared the same sex chromosome, including the early-diverging species *Dictyota dichotoma*. Based on these data, we conclude that the recombination suppression event that gave rise to the U/V sex chromosomes occurred at least >250 Mya, at the origin of the Phaeophyceae[15,17]. We note that neither *Fucus serratus* nor the monoicous (co-sexual) species *Chordaria linearis* and *Desmarestia dudresnayi* have a U/V sexual system, yet they still conserve the chromosome that is homologous to the U/V sex chromosome in the dioicous species (hereafter referred to as 'sex-homolog').

In the outgroup *S. ischiensis*, we found very low synteny with the sex-homolog and patterns of fusion-with-mixing[18] between the homologs of chromosomes 4 and 9 as well as between chromosomes 23 and 24 of *D. dichotoma* (**Fig. 1A; Fig. S1**). Such fusion-with-mixing events are believed to represent irreversible states of chromosome evolution[18], and therefore, *S. ischiensis* likely represents a divergent karyotype, rather than a proxy karyotype of the last brown algal common ancestor. Because sexual reproduction of *S. ischiensis* has never been observed in culture, its sexual system is currently unknown.

We next examined the SDRs on the U and V sex chromosomes by comparing male and female genomes for all dioicous species (see methods). The V-SDR differed markedly across species, both in terms of gene content, total size and relative size compared to the pseudo-autosomal region (PAR), a region that is homologous across sex chromosomes and is involved in their recombination during meiosis (**Fig. 1B, Table S1**). We found the smallest SDR sizes in the Ectocarpales (*S. promiscuus* and *Ectocarpus* sp.7) (**Fig. 1B-C**), and noticed that genes that correspond to PAR genes in *Ectocarpus.* sp.7 and *S. promiscuus* were present in the V-SDR of early-diverging brown algae such as *D. dichotoma* and *D. herbacea*. Similarly, the size of the female SDR is different in *Ectocarpus* sp. 7 and *D. herbacea,* with a subset of PAR genes in *Ectocarpus* sp. 7 also incorporated in the SDR of *D. herbacea* (**Fig. 1C**). In addition, the V-SDR of *D. herbacea* and *D. dichotoma* had undergone

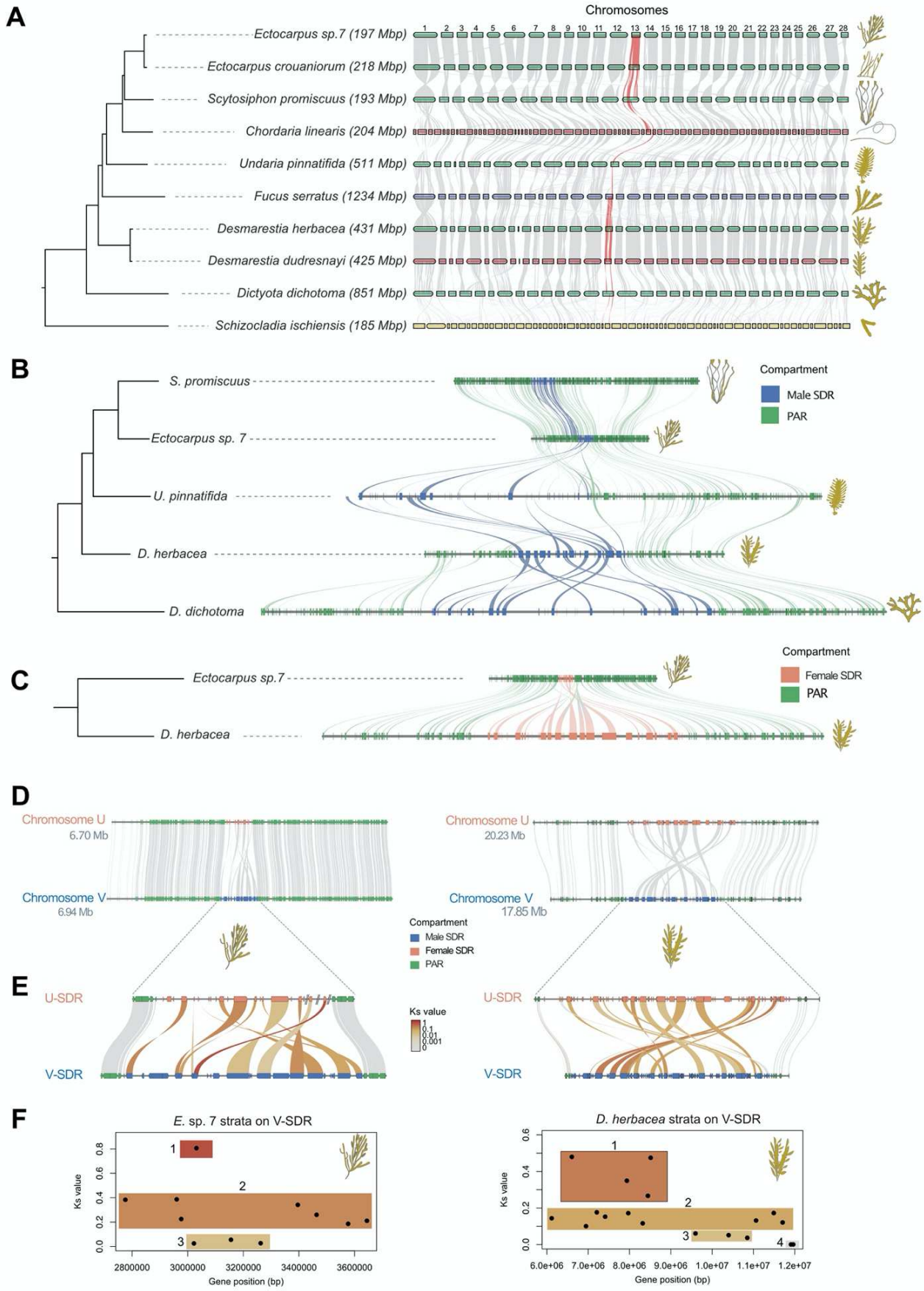

Figure 1. Brown algae share an ancestral sex chromosome. (A) Macrosynteny plot between brown algal genomes of six dioicous species (green), two monoicous species (red), one dioecious species (blue) and the outgroup species (yellow). The syntenic blocks corresponding to the V sex chromosome are highlighted in red. The size of each genome is displayed inside brackets. (B) Microsynteny plot of the V chromosomes in five dioicous species, showing the regions that belong to the male sex-determining region (blue) and the PAR (green) for each species. (C) Microsynteny plot of the U chromosomes in two dioicous species, showing the regions that belong to the female sex-determining region (peach) and the PARs (green) for both species. (D) Microsynteny plot between the U and V chromosomes of *Ectocarpus sp. 7* and *D. herbacea*. (E) Synteny between the U and V gametologs in the SDRs of *Ectocarpus sp. 7* and *D. herbacea*. The matching shades within the SDR are colored according to the number of synonymous substitutions per synonymous site (*Ks*) for each gametolog pair. (F) Identification of evolutionary strata in the male SDR of *Ectocarpus* sp. 7 and *D. herbacea* according to the *Ks* values of gametolog pairs and the position of the male (V) genes in the SDR.

rearrangements and inversions whereas the SDR in *U. pinnatifida* had relocated from the center to the periphery of the V chromosome (**Fig. 1B**). Furthermore, we identified a large inversion in the female SDR of *Ectocarpus* sp. 7 and *D. herbacea* (**Fig. 1C**) and between the V and U chromosomes within the same species (**Fig. 1D**). Taken together, and despite an overall high level of macrosynteny, our findings reveal that SDRs in brown algae undergo dynamic structural changes through evolution.

Upon analysis of synonymous substitutions per site (*Ks*) across male and female gametologs, we noticed that the SDR of *Ectocarpus* sp. *7* is composed of several highly-divergent gametologs in two (presumably older) 'evolutionary strata' and three gametolog pairs in a more recent evolutionary stratum (**Fig. 1D-E, Table S2**). In contrast, the SDR of *D. herbacea* contained more gametolog pairs with relatively high *Ks* values and more recently diverged SDR genes, forming at least four 'evolutionary strata' (**Fig. 1D-E**). The gametolog *Ks* values are broadly concordant between the orthologs in *Ectocarpus sp. 7* and *D. herbacea* (**Table S2**), indicating that the accumulation of synonymous substitutions can be considered a proxy of evolutionary distance in comparable species. Nonetheless, the SDR *Ks* values do not group together as they do in XX/XY sexual systems, where they form well-defined 'evolutionary strata'[19]. Instead, the shuffling of gene order within the SDR and dynamic movement of genes in and out of the SDR[20,21] likely diluted the ancestral SDR arrangement in the extant species, limiting our ability to clearly define evolutionary strata based on gene position (**Fig. 1F**). The occurrence of recently evolved evolutionary strata in *D. herbacea* combined with an inverted pattern between male and female is consistent with an expansion of the SDR in brown algae caused by nested inversion events that suppress recombination. Indeed, when comparing *Ectocarpus* sp. 7 and *E. crouaniorum*, we note that the male SDRs are inverted with respect to each other (**Fig. S2**), indicating that inversions are persistent even between closely-related taxa.

Together, these results indicate that despite the macro-synteny stability across brown algal genomes, the structure of U/V sex chromosomes is highly divergent. The frequent chromosomal inversions and gene movement into and out of the SDR likely played a pivotal role in the evolution of the brown algal SDRs.

Lineage-specific expansion of the SDR is associated with increased gamete dimorphism

The presence of larger SDRs in early diverged brown algae such as *D. dichotoma* and smaller SDRs in later diverged orders such as Ectocarpales could indicate that gene loss may have the reduced SDR physical size. However, different brown algae lineages could also have independently expanded their SDRs, while the SDR size of Ectocarpales remained stable. To understand SDR size dynamics across species, we performed an ancestral state reconstruction of SDR gene content. Considering that U and V are expected to evolve similarly due to their inheritance patterns[20,22,23], and overall better data quality for male species, we focused our investigation on the V-chromosome. We found that V-SDR evolution is mostly driven by lineage-specific expansions of an ancestral SDR that contained a small number of genes in the common ancestor (**Fig. 2A**). Remarkably, within the ancestral state reconstruction, male gametologs with higher *Ks* values were mostly supported as ancestral male SDR genes, whereas male gametologs that were independently acquired into the SDR displayed the lowest *Ks* values in *D. herbacea* (**Table S2,** see **Fig. 1E**). However, we note that some gametologs did not follow this pattern, highlighting that defining evolutionary strata for brown algae based solely on *Ks* values is challenging.

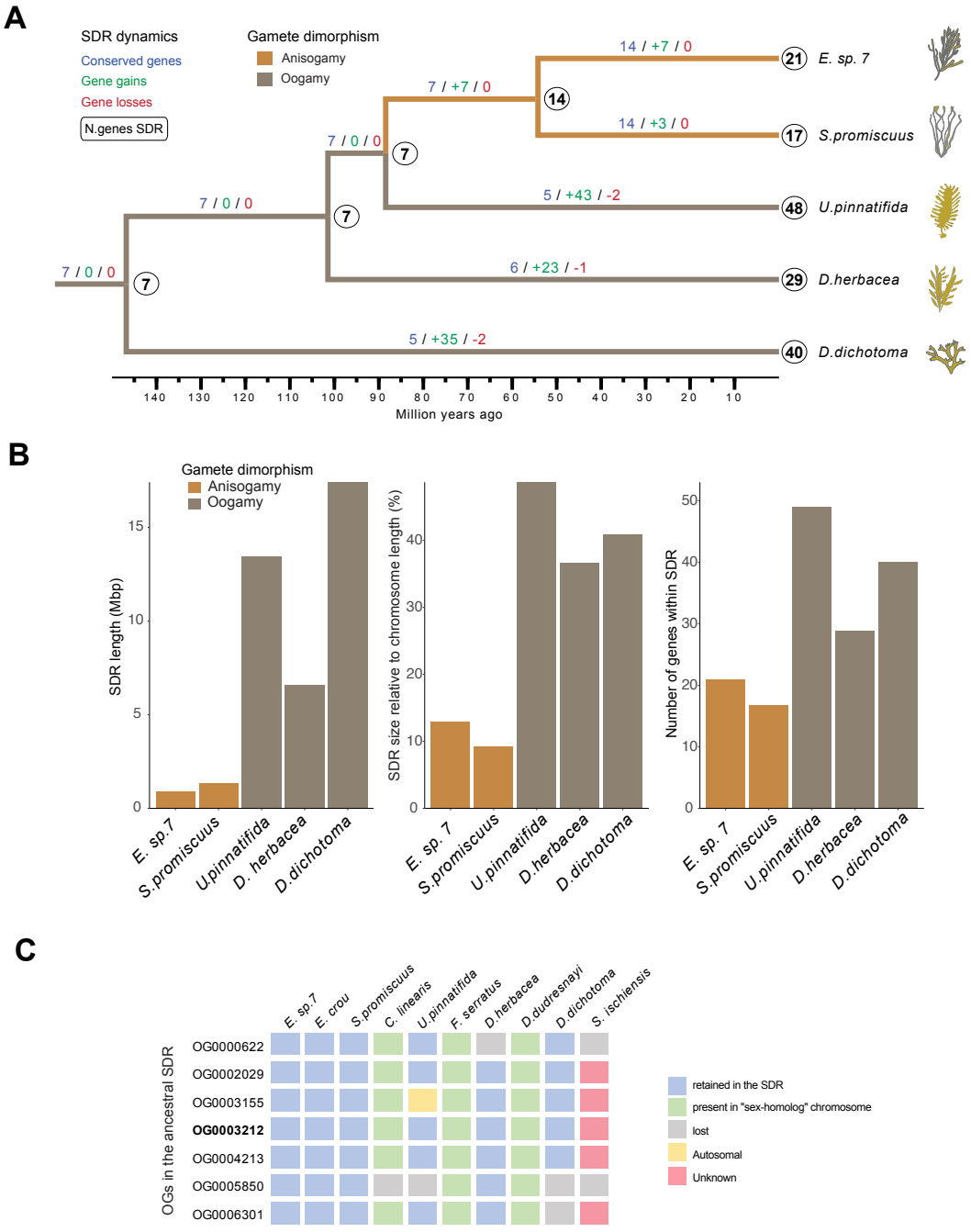

Figure 2. Lineage-specific expansion of the V-SDR is associated with increased sexual dimorphism. (A) Ancestral state reconstruction of V-SDR gene content across the brown algal phylogeny, showing the expected number of genes in the SDR (circles on the right side of each node), the number of SDR genes that were retained compared to the previous node (blue), the genes that were incorporated into the SDR (green) and the genes that were lost or that were translocated outside of the SDR (red). The ancestral state reconstruction of gamete dimorphism (based on [14]) shows a transition from oogamy to anisogamy in the Ectocarpales alongside with changes in the SDR gene content. (B) Differences in the size of the male SDR between brown algal species based on the total sequence length, the relative size of the SDR compared to the length of the V chromosome and the number of protein-coding genes retained within the SDR. The bars are colored according to the level of gamete dimorphism in each species (based on [14]). (C) Schematic view of the location of the 7 ancestral V-SDR genes (blue: retained in the SDR; green: contained within the pseudoautosomal region or the sex-homolog; yellow: autosomal; red: Unknown genomic localition; grey: lost). Bold: *HMG-sex*. See also Table S4.

The SDRs of *Ectocarpus sp. 7* and *D. herbacea* contain genes that are homologous between the U and V chromosomes, suggesting that these haplotypes descend from a common ancestral autosomal region. Even though SDR gene numbers differ, they share the same ratio of roughly 50% gametologs and 50% sex-specific (*i.e.* genes only found on the male or female SDR; **Table S3**). In contrast, the male SDR of *D. herbacea* contains a higher number of sex-specific genes, but this excess was driven by a recent insertion of viral sequences into the male SDR (**Table S3**). Thus, genes present in one sex only were either acquired after the divergence of the U and the V regions or lost by the counterpart haplotype.

Intriguingly, SDR size was strongly associated with the level of gamete sexual dimorphism for the five studied species. Specifically, oogamous species, in which male and female gamete size differs significantly (e.g., *U. pinnatifida* or *D. herbacea*) have larger SDRs than species with modest gamete size differences (anisogamy, e.g. *Ectocarpus sp. 7*) (**Fig. 2A-B**). Importantly, we noticed that most of the SDR genes in the oogamous species were acquired independently for each lineage, hence, expansions likely occurred independently and concomitant with changes in gamete size (**Fig. 2A; Fig. S3**). Previous work suggested that oogamy is ancestral in brown algae[14] and that a transition from oogamy towards anisogamy occurred in the Ectocarpales. However, our observations rather indicate an independent acquisition of oogamy from an anisogamous ancestor (**Fig. 2A-B**). In contrast, the SDR of the Ectocarpales acquired fewer genes, and likely resembles the ancestral SDR state more closely.

In our initial reconstruction, we retrieved 12 genes that were present in the ancestral V- SDR (see methods). However, we found on our gene tree analyses that five of those genes were present in several brown algal species as parallel and independent SDR expansions (**Fig. S3**) and that the ancestral SDR contained seven genes (**Fig. 2C**). These seven genes comprised six gametologs and one male-restricted gene, all associated with crucial aspects of sex determination (**Fig. 2C, Table S4**). For example, the master male sex-determining gene *HMG-sex* (Luthringer et al., in review) is always present in the male SDR, consistent with it being the initial trigger that favored progressive recombination suppression through inversions. Another gene encodes a transmembrane protein with a putative sugar-binding and cell-adhesion domain (Ec-13_001840 in *Ectocarpus* sp.7), identified as a gametolog in the female SDR (Ec-sdr_f_000170). Considering that gamete recognition in brown algae is mediated by unknown carbohydrate-binding receptors[24] this gene is an interesting candidate for this function. In addition, we found a homolog of STE20 serine/threonine kinase (Ec-13_001910 in *Ectocarpus* sp.7) as part of the ancestral SDR in brown algae, whose homolog in yeast is involved in the transcriptional activation cascade of mating-type genes after pheromone recognition[25]. Other ancestral SDR genes associated with signal transduction include a casein kinase (Ec-13_001990), a MEMO-like domain protein (Ec-13_001810) and a GTPase activating protein (Ec-13_001710).

The six genes that belong to gametolog pairs showed no evidence of degenerative evolution and remained functional in both male and female *Ectocarpus.* In *D. herbacea*, four of the genes are retained in the male and female SDR, while the fifth had become male-specific and the sixth completely lost in both sexes, indicative of a mild level of degradation. Taken together, and despite being evolutionary old, haploid sex chromosomes in brown algae undergo less gene loss relative to XX/XY and ZW/ZZ systems, and evolve mainly by gene gain (**Fig. 2A**).

Consistent with roles in sexual development, the majority of SDR genes (58-100% of SDR genes depending on the species) were expressed at substantial levels (log2(TPM+1) > 1) during the fertile gametophyte stage

(**Table S5**). Furthermore, we conducted a comparative analysis of gene expression (mature gametophyte phase), in which we contrasted genes that became independently acquired in the sex-determining regions in each species with the single-copy autosomal paralogs present across different species. Notably, the expression levels of the newly sex-linked genes remain comparable to their autosomal counterparts (**Fig. S4**), suggesting that the autosomal biological activity may become co-opted to perform a male-specific function in the V-SDR genetic setting.

Interestingly, whilst the size of the SDR correlated well with the level of gamete dimorphism (see above), we found no correlation between the amount of autosomal sex-biased gene (SBG) expression and differences in gamete size across males and females (**Table S6**), in agreement with a study of a small subset of brown algal species[26]. Notably, species with low sexual dimorphism and smaller SDRs actually exhibited the highest proportion of SBG (**Fig. S5A**). Intriguingly, we observed an enrichment of male-biased genes (MBG) within the PAR across all species, except in *D. dichotoma (***Fig. S5B**).

Most of the ancestral SDR genes were also present in the genomes of algae that do not have a U/V sexual system, namely the monoicous species *C. linearis* and *D. dudresnayi*, the dioecious species *F. serratus* and in the outgroup *S. ischiensis* (**Fig. 2C, Table S4)**. Hence, the ancestral SDR genes may play important roles even in the absence of a U/V sex-chromosome system. Notably, all the non-dioicous brown algal species retain most of these genes on their sex-homolog chromosomes, as expected from the strong conserved synteny in Phaeophyceae. However, the SDR orthologs in *S. ischiensis* are scattered throughout the genome, possibly as a consequence of fusion-with-mixing events.

Altogether, our analyses indicate that the U/V system in brown seaweeds is highly dynamic, and evolved mainly by lineage-specific gene gains that took place concomitant with increased sexual dimorphism. The brown seaweed U/V system appears to have undergone sparse degeneration. We detect a set of genes that has been conservatively sex-linked across the evolution of the dioicous brown algae, implying that these genes have a key role in sex determination and/or differentiation.

Structural and evolutionary features of haploid sex chromosomes

Our chromosome-level assemblies allowed us to evaluate the genomic characteristics that differentiated the SDR and the PARs from the rest of the genome. When compared to the autosomes, and as typical of non-recombining regions[27], protein-coding genetic sequences (*i.e.*, exons) were depleted in brown algal SDRs (**Table S7**) whereas repetitive elements were enriched (**Fig. 3A, Table S8**). Within the repetitive element classification, we found that 'unclassified' transposable elements in the sex chromosome were enriched in *S. promiscuus*, and to a lesser extent, in *Ectocarpus* sp. 7 (**Fig. 3A; Fig. S6; Table S9**). In contrast, the SDR of species that experienced genome expansions (*U. pinnatifida*, *D. herbacea*, *D. dichotoma*) were colonized by LTRs elements, which appear to be the main drivers of genome expansion in brown algae (**Fig. 3A; Fig. S6; Table S9**).

In addition, we detected fewer conserved sex chromosome orthologs between species than expected by chance (Chi-squared test, p-value < 10^{-4}, **Table S10**), an observation possibly related to increased number of evolutionary young (taxonomically-restricted) genes (TRGs) in these regions, as we demonstrated previously for *Ectocarpus* sp.7[28]. Therefore, we examined the cause of reduced sex chromosome synteny by performing a phylostratigraphic analysis[29,30] to evaluate the relative ages of each gene. We found that genes in the

different age categories were not randomly distributed across chromosomes (Kruskal-Wallis test, p-values $<10^{-40}$ for all species). Consistently, the sex chromosomes of dioicous species were enriched in young genes and depleted in older, highly conserved genes (**Fig. 3B**; **Table S11**). Intriguingly, the gene age categories that were enriched in the sex chromosomes belong to taxonomic categories that are not shared between the analyzed taxa (species, genus and family-level gene ages; **Figs. S7-S11**), suggesting that the pattern of TRG enrichment in the sex chromosomes arose independently in each lineage.

In a previous study, we proposed a theoretical model to explain how TRG accumulation through generation-antagonistic selection favors the retention of young sporophyte-beneficial loci in the sex chromosome of *Ectocarpus*[28]. Here, we examined if genes with a generation-(sporophyte)-biased expression accumulated in the sex chromosome of the other dioicous species. Indeed, we found that not only were generation-biased genes (sporophyte-biased, as reported in [28]) enriched in the sex chromosome of *Ectocarpus*, this pattern was also obvious in the sex chromosome of the kelp *U. pinnatifida*. In contrast, the pattern was less clear in *S. promiscuus* and *D. dichotoma* (**Table S12).** Importantly however, we note that these latter species are unlikely to experience 'generation-antagonism' either because both generations are phenotypically similar (*D. dichotoma*), or the sporophyte generation is significantly reduced compared to the gametophyte generation (*S. promiscuus*)[14,26].

New genes can emerge from ancestrally non-genic regions through mutation(s) that either create coding potential through *de novo* birth processes[31], through selection-driven sequence divergence that changes the gene beyond the point of recognition to other homologs[32] or via a constant accumulation of neutral mutations leading to failure of detecting homology[33]. To explore these possibilities, we first estimated the synonymous substitution rate (*Ks*) between orthologs in other closely-related species and searched for differences in *Ks* values between chromosomes and between the different genomic compartments (SDR, PAR, autosomes). We reasoned that if synonymous mutations behave neutrally[34,35], then the rate of synonymous substitution (*Ks*) can be employed as a proxy for the point mutation rate[36,37]. Consistently, the V sex chromosomes for all dioicous brown algal species were associated with higher *Ks* values (**Fig. 3A**; **Table S13**), suggesting that the mutation rate is substantially higher in these genomic regions compared to autosomes. We were intrigued to see that the enrichment of young genes and higher *Ks* values appear to be localized in the PARs of *Ectocarpus* sp. 7 and *S. promiscuus* (**Fig. S7-S8**), but noted that this pattern extends to the entire sex chromosome in species with large SDRs such as *U. pinnatifida*, *D. herbacea* and *D. dichotoma* (**Fig. S9-S11**).

Together, these analyses indicate that brown algal U/V chromosomes accumulate transposable elements and have decreased gene density, as has been observed for the non-recombining regions of XX/XY and ZW/ZZ systems. They also appear to have the remarkable ability to spawn gene novelty, likely due to their unique structural and evolutionary features.

Transition from haploid to diploid sexual systems in the Fucales

While ancestral sex determination in most brown algae is based on haploid U/V sex chromosomes, several algal lineages have independently lost this system and evolved either a diploid sex determination system (XX/XY)[38] or monoicy (*i.e.*, in which the same haploid individual can produce male and female gametes)[26]. We therefore investigated the evolutionary trajectory of brown algal genomes following the 'loss' of the U/V sex chromosome system.

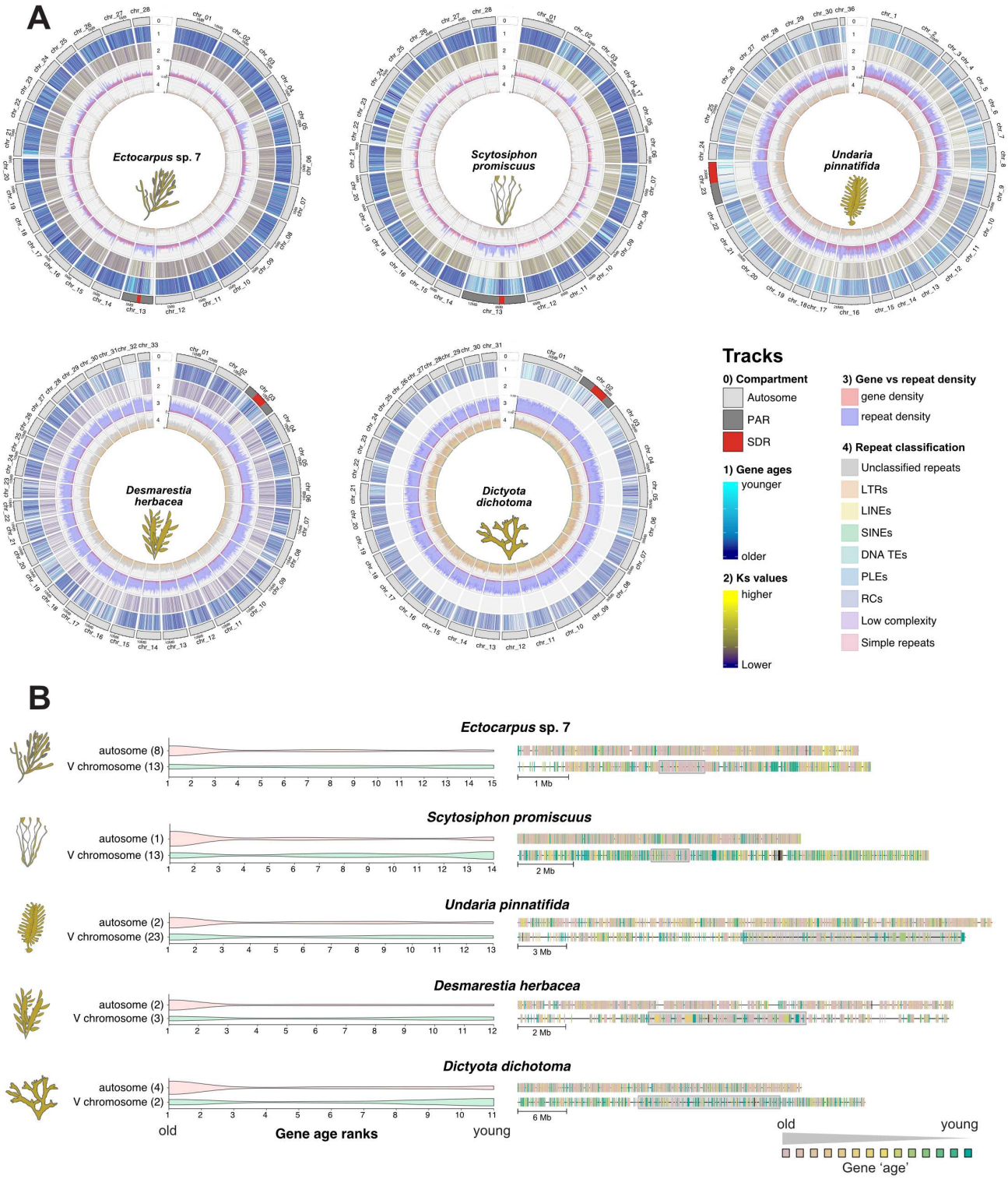

Figure 3. Genomic features of sex chromosomes compared with autosomes. (A) Circos plots displaying tracks for the following genomic features: 0) chromosome compartments: autosomes, PARs and SDR; 1) relative gene ages, 2) *Ks* values, 3) proportion of gene density (red) against repeat density (blue) and 4) repetitive element classification. (B) Violin plots and physical distribution of relative gene ages across one autosome and the V sex chromosomes of *Ectocarpus* sp. 7, S. *promiscuus*, *D. herbacea*, *U. pinnatifida*, *D. dichotoma*. The SDR of the sex chromosome is highlighted with a grey shadow.

The Fucales, which are important components of the coastal areas across the globe, are the one of the two brown algal lineage that transitioned to a diploid life cycle[39], with many Fucales species having separate sexes in the diploid stage of the life cycle (XX/XY sex determination[38]). We first set out to identify the Y chromosome of the dioecious *Fucus serratus*. Verbal models state that transition from haploid U/V systems to diploid sexual systems should occur via a stage of epigenetic sex determination, followed by emergence of a neo-sex chromosome[2]. Therefore, it is possible that the ancestral V chromosome does not necessarily correspond to the sex chromosome of the Fucales. In order to identify sex-linked regions in *F. serratus*, we employed a range of sex chromosome detection pipelines including high coverage genome sequencing of males and females, combined with RAD-seq data generated for 12 males and 12 females from a field population (see methods for details). None of these efforts led to the identification of sex-linked sequences, implying that the SDR of *F. serratus* is likely to be very small and undifferentiated. This result is consistent both with a very young Y chromosome having arisen in the Fucales following the transition to diploid life cycle, and also with the high turnover in terms of sexual system in this lineage[40]. Indeed, theory predicts that switching to monoecy from dioecy is only possible if the SDR is not very differentiated[41].

Synteny analysis (see **Fig 1**) indicated that *F. serratus* retains a chromosome that is homologous to the V chromosome of the ancestral U/V species. In addition, the conserved SDR genes from the ancestral U/V systems included the V-specific male-determining gene (*HMG-sex*; Luthringer et al., in review) and several other V-linked genes (see **Fig. 2C**). Although none of the ex-SDR genes were sex-linked in *F. serratus*, *HMG-sex* and four additional ancestral SDR genes (homologs of Ec-13_001990, Ec-13_002040, Ec-13_001840 and Ec-13_002040 in *Ectocarpus* sp.7) had a strong male-biased expression pattern (**Fig 4A**, **Table S14**), being silenced in *F. serratus* females. Remarkably, these ancestral V-SDR genes were also silenced in female strains of three other Fucales species (*Ascophyllum nodosum*, *Fucus ceranoides* and *Fucus vesiculosus*; **Table S15**). Thus, whilst the ancestral V-linked genes are no longer sex-linked in the Fucales, they are still likely participating in the genetic cascade of male sex determination and/or differentiation.

Consistent with the lack of a differentiated sex chromosome, we did not observe any specific structural feature in any of the chromosomes of *F. serratus,* which transitioned from U/V to an XX/XY dioecious system approximately 65 Mya[17]. In particular, we did not observe any trace of TRGs accumulating in *Fucus* chromosomes (as described above for U/V systems) nor higher *Ks* values or higher TE content on the sex-homolog or in any other chromosome (**Fig.4B; Fig. S12; Tables S7-S11, S13**).

Fate of U/V sex chromosomes following transition to co-sexuality

Next, we used our genomic datasets to assess the fate of sex chromosomes once they are in a co-sexuality context and to understand the origin of monoicous algal species. We found that the large majority of genes in the sex-homologs of both *C. linearis* and *D. dudresnayi* are male-derived, indicating that they originate from a male genomic background (**Fig. 5A-B**). In *C. linearis*, fifteen SDR orthologs have a male origin and only two a female origin (**Fig. 5A**, **Table S16**). The sex-homolog of *C. linearis* contains several rearrangements that span both the regions belonging to the ancestral PARs and the ancestral SDR (**Fig. 5A**). Most of the SDR orthologs remained in a syntenic region within the sex-homolog, with one male ortholog being translocated within the same chromosome (ortholog of Ec-13_001490) and another male ortholog translocated to a different chromosome (ortholog of Ec-13_002020). Notably, most SDR orthologs lost during the transition to monoicy display their corresponding gametologs or retain closely-related autosomal paralogs

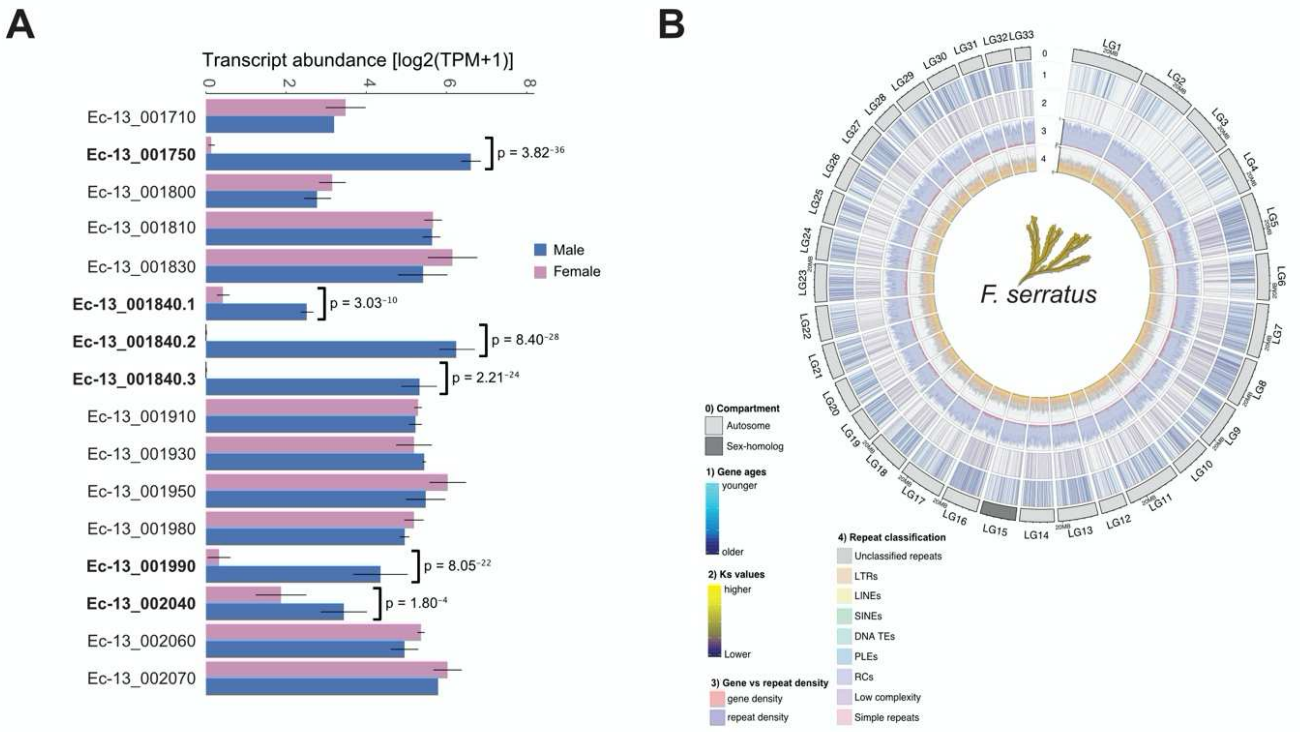

Figure 4. Transition from haploid to diploid sex determination. (A) Expression of ancestral V-SDR genes in the diploid species *F. serratus*. Gene expression of mature algae (using 3 males and 3 females, see methods) is given as log2(TPM+1) and bars represent standard deviation of the mean. (B) Circos plot of *F. serratus* displaying tracks for the following genomic features: 0) chromosome compartments: autosomes and sex-homolog; 1) relative gene ages, 2) *Ks* values, 3) proportion of gene density (red) against repeat density (blue) and 4) repetitive element classification. The sex-homolog has lost the genomic footprints of a sex chromosome, with no distinguishing patterns in its sex-homolog or in any other chromosome (see Fig. S12 and Tables S7-S11, S13).

within the genome of *C. linearis* (**Table S16**). Nonetheless, all these genes belong to multigene families in both *Ectocarpus* sp.7 and *C. linearis*. Therefore, it remains unclear if the expression of the lost SDR genes in *C. linearis* would be compensated by a gene family member.

Interestingly, the only two SDR orthologs of female origin are framed by PAR orthologs that separate them from the other SDR-derived genes. Together, these observations indicate that *C. linearis* descended from a male genomic background that acquired its female-derived SDR genes through at least three non-homologous recombination events (**Fig. 5A**).

Similarly, the sex-homolog in *D. dudresnayi* also includes chromosomal rearrangements, with at least two inversion events within the region that is homologous to the male SDR in *D. herbacea* (**Fig. 5B**), and with 20 SDR orthologs of male origin and only 5 of female origin (**Table S17**). The two most recently acquired SDR genes in *D. herbacea* are also present in the monoicous *D. dudresnayi*, but these two genes were integrated into the SDR of *D. herbacea* after diverging from *D. dudresnayi*. Similarly, we found at least three viral insertions in the male SDR of *D. herbacea* that are absent in the sex-homolog of *D. dudresnayi*, suggesting that these insertions are male-exclusive and occurred after the two species had diverged. As with *C. linearis*, most of the genes that were lost during the transition to monoicy had a putative gametolog or a paralog compensation (**Table S17**). One of the female SDR genes in *D. dudresnayi* appears close to the PAR region in a similar fashion to *C. linearis*, while two other female genes were translocated and conserved elsewhere in the genome.

Next, we examined the expression pattern of ancestral male SDR genes present in the sex-homologs of *C. linearis* and *D. dudresnayi*. Both *C. linearis* and *D. dudresnayi* retain a copy of *HMG-sex*, confirming its crucial role in the male developmental pathway in the monoicous species (Luthringer et al., in review). Remarkably, these genes are expressed during the reproductive stages of both species **(Table S18)**, suggesting that ancestral SDR genes play a key role in reproduction - even in the absence of a U/V sex-chromosome system. Interestingly, all non-dioicous brown algal species retain most of these genes in a strongly conserved synteny pattern on their sex-homolog chromosomes. Conversely, most of the female genes were lost in the monoicous species, with the exception of one female gene, orthologous to a protein with unknown function in *Ectocarpus* sp.7 (Ec-sdr_f_000220.1) that is actively expressed during fertility (**Table S5**).

Together, these results indicate that monoicous species require a male genomic background to retain all the necessary features of a functional sexual phenotype and likely arose from an ancestral male that acquired female SDR genes via ectopic recombination.

Lastly, we examined if high TE content, TRG enrichment and high *Ks* values on the sex chromosome are features exclusive to U/V sex-determination systems or if they form a broader pattern common to all sexual systems in brown algae. Indeed, we detected TE content enrichment and younger TRGs on the sex-homolog in *D. dudresnayi*, although the *Ks* values were not higher in this chromosome when compared to the rest of the genome (**Fig. 5C; Fig. S13; Tables S7-S11, S13**). Due to the recent loss of the U/V system in *D. dudresnayi*, its evolutionary footprint is still present in the sex-homolog, such as TRG enrichment, although the evolutionary dynamics is gradually being lost after splitting from *D. herbacea* and becoming monoicous, as shown by the *Ks* values.

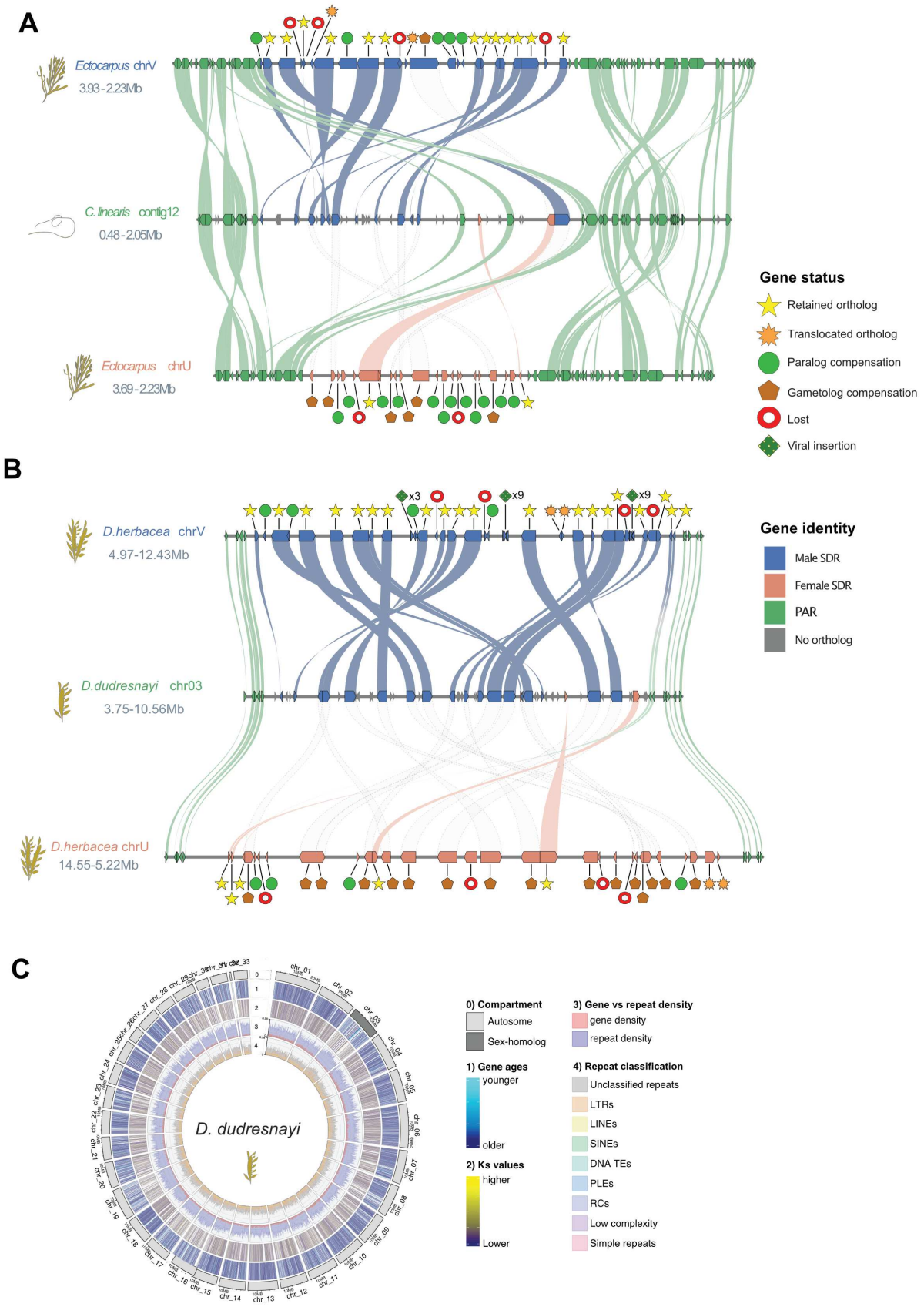

Figure 5. Fate of sex chromosomes during transitions from dioicy to co-sexuality. (A) Comparison of the sex-homolog in *C. linearis* against the U and V chromosomes of *Ectocarpus* sp. 7. (B) Comparison of the sex-homolog in *D. dudresnayi* against the U and V chromosomes of *D. herbacea*. The color code represents the identity of the genes alongside the chromosomes, while the shapes represent the evolutionary fate of each SDR gene in the monoicous genome. The matching shades between the SDRs and the sex homolog are either color-coded by their ancestral background or they appear as transparent dotted shades if the gametolog of the other sex was retained. (C) Circos plot of *D. dudresnayi* displaying tracks for the following genomic features: 0) chromosome compartments: autosomes and sex-homolog; 1) relative gene ages, 2) *Ks* values, 3) proportion of gene density (red) against repeat density (blue) and 4) repetitive element classification. *D. dudresnayi* retains the gene cradle pattern in the sex-homolog, but its *Ks* values are no longer different to those of the other chromosomes (see also Fig. S13 and Tables S7-S11, S13).

DISCUSSION

Structure and synteny level of brown algal sex chromosomes

Our genomic and experimental data allowed us to identify the sex chromosomes or sex-homologs in nine representative brown algal species and one outgroup. We revealed a high degree of synteny conservation across species (with the exception of the outgroup *S. ischiensis*), consistent with previous analyses in Metazoans, where synteny is highly conserved alongside the emergence of animal multicellularity[42]. Macrosynteny conservation between distantly-related species is thought to be maintained through an interplay between constrains in cis-regulatory interactions within chromosomes and selection against disruptions during meiotic pairing[18,42,43], mechanisms that may also be playing a role in brown algae as they also evolved complex multicellularity.

Despite synteny conservation of brown algal autosomes, the evolution of the sex chromosomes, and particularly the SDR in the U/V chromosomes, is structurally dynamic. Chromosomal inversions occurred frequently throughout the brown algal phylogeny and appear to have played a pivotal role in the evolution of brown algal SDRs. Chromosomal inversions were likely responsible for the initial recombination suppression in the proto-sex chromosomes, as well as the subsequent expansion events of the SDR into the bordering PARs. The structural dynamism in the SDR is likely driven by TE-mediated chromosomal rearrangements[44], since the sex chromosome is enriched in TEs relative to the rest of the genome. As described in other systems, including mating type chromosomes in fungi[45,46], TE accumulation was likely a consequence of the initial recombination suppression in the SDR[47] which possibly initiated a positive feedback loop between the accumulation of TEs in the sex chromosome and the subsequent rearrangement and expansion of the SDR.

Sexual dimorphism and the evolution of the SDR

Classical XX/XY and ZW/ZZ sex chromosome models suggest that sexual dimorphism may be shaped by sexually antagonistic selection, which in turn may drive the expansion of the SDR, favoring the evolution of new evolutionary strata[48,49] although other models have also recently been proposed[50–53]. We found that brown algal species with higher gamete sexual dimorphism are prone to expand their SDR boundaries, which would be consistent with higher sexual dimorphism involving a larger number of genes under sexually antagonistic selection[54]. Coincidentally, species with larger SDRs and higher level of gamete dimorphism are also morphologically more complex compared to the species with small SDRs[15]. This may reflect an interplay between morphological complexity, the retention and acquisition of sex-specific genes in the SDR and the emergence of sexual dimorphic traits.

Oogamy is thought to be the ancestral state in brown algae, but this trait seems to be labile[14]. Our analysis is concordant with a scenario in which several transitions to oogamy occurred independently in different lineages from a less dimorphic ancestor, and that the increase in gamete dimorphism was accompanied by expansion of the sex locus. Levels of gamete dimorphism were correlated with larger SDRs but there was no correlation with the levels of sex biased gene expression – therefore, our results suggest that sexual differentiation in these organisms may be driven by genes within the SDR to a higher degree than by autosomal sex-biased gene expression. Previous studies in other brown algae[26] and in plants[55] support this idea, since they too did not find a link between sex-biased gene expression and level of sexual dimorphism.

U/V accumulate TEs but show mild genetic degeneration

The current models of XX/XY and ZW/ZZ systems state that the suppression of recombination between sex chromosomes is followed by the accumulation of mutations and degeneration of the heterozygous chromosome (Y or W) due to a lower efficacy of selection in non-recombining regions of the genome[56], although more recent models of degeneration by regulatory evolution[57] or neutral models[50,52] do not require selective interference nor sexual antagonism to explain sex chromosome differentiation. Our analysis of the U/V chromosomes reveal important differences to XX/XY and ZW/ZZ evolutionary trajectories. U/V structure changes quickly throughout time through multiple inversion events, the accumulation of TEs and reduction of gene density. While the accumulation of TEs can be explained by the suppression of recombination in the SDR, the low gene density is not necessarily related with degenerative evolution and gene loss. Rather, it seems that the SDR expanded by an accumulation of TEs, which moved the genes apart from each other, lowering the overall gene density. Unlike the Y and W chromosomes, gene loss events in the U/V SDRs are an uncommon phenomenon. We found that *Ectocarpus* sp. 7 retained gametolog pairs for all the six ancestral V-SDR genes, while *D. herbacea* also retained most of these genes as gametologs. These data are indicative of a mild degeneration rate of the U/V systems, as previously predicted by Bull[22]. Contrary to XX/XY and ZW/ZZ systems, our ancestral state reconstruction analysis shows that the SDR on every brown algal lineage had more gene gain events than losses. Considering that U/V chromosomes perform their sex-determining activity during the haploid stage, SDR genes are expected to be under haploid purifying selection, leading to a more efficient purge of deleterious mutations compared to diploid systems[58,59].

Surprisingly, the accumulation of TEs appears to behave differently in the U/V sex chromosomes when compared to the autosomes. *Scytosiphon* and *Ectocarpus* have the smallest genome sizes in our analysis and display an enrichment of unclassified TEs, particularly in the SDR but also extending into the PARs. In contrast, species with larger genomes no longer have this pattern, and it is even reversed as LTRs expanded throughout the genome. While RNA transposons like the LTRs have an unbiased insertion pattern throughout the genome, DNA transposons display local hopping, meaning that they tend to insert themselves in the vicinity of the donor locus[60]. It is plausible that these unclassified TEs represent novel or degraded DNA transposons that flourished in the SDR and subsequently expanded to the PARs through local hopping. This signal would be subsequently lost in the species with large genomes, as LTRs started colonizing the genome, with a higher conservation in the SDR due to suppressed recombination.

U/V sex chromosomes are gene nurseries

We found strong signals of young TRG accumulation on the U/V sex chromosomes of the dioicous brown algae, extending previous observations in *Ectocarpus* sp. 7[28]. Therefore, U/V sex chromosomes may function as 'cradles' for evolutionary novelty. What could be the mechanism underlying the U/V sex chromosomes 'cradle' pattern? Sex chromosomes in *Ectocarpus* are enriched in repression-associated chromatin marks (*e.g.*, H3K79me2) associated with transposons[61], likely to suppress TE transposition in this chromosome. Heterochromatic regions have been suggested to display higher mutation rates due to the limited access of the DNA repair machinery to correct errors during replication[62]. Accordingly, we found consistently higher mutation rates in the sex chromosome. It is therefore possible that the TE and heterochromatic landscape of the sex chromosomes favor the emergence of young TRGs. These genes would

then be retained in the sex chromosome by 'generation-antagonistic selection', which would selectively maintain genes that bring an advantage to the sporophyte generation[28]. This mechanism requires differential selective pressures between the gametophyte and the sporophyte stages, and would therefore require a dimorphic life cycle where gametophyte and sporophyte generations would have considerable phenotypic differences. Notably, *D. dichotoma does* not display generation dimorphism[14], and, accordingly, does not display a clear pattern of sporophyte-biased gene expression enrichment in the sex chromosome. Furthermore, *S. promiscuus* has a highly reduced (in terms of size and morphological complexity) sporophyte stage[14] where selective pressures should be limited, which is the other species where we could not find sporophyte-biased gene expression in the sex chromosome. Thus, the gene cradle pattern could be reinforced through generation-antagonistic selection, but higher mutation rates alone appear to be sufficient to initiate this pattern in species without sporophyte-biased gene expression.

The gene cradle pattern is visible only in species with U/V sex chromosomes, and it is considerably diluted in *D. dudresnayi* where the transition to co-sexuality occurred very recently. Moreover, the cradle pattern is absent in *F. serratus.* The Fucales lineage diverged from the ancestral U/V brown algae 65 Mya[17], suggesting that losing the U/V system for an extended amount of evolutionary time results in the disappearance of the gene cradle pattern. Even though there are no clear markers with which to define the Y chromosome in *F. serratus*, none of its chromosomes are overrepresented in TRGs. Therefore, the gene cradle pattern seems to be very specific to the U/V system in brown algae and to the type of life cycle of these organisms.

While details of the proximate and evolutionary mechanisms underlying TRG emergence remain to be defined[31–33], our data suggest a complex interplay between complex life cycles, heterochromatic landscape, presence of TEs, and higher mutation rates that would favor the emergence of novelty.

Genomic consequences of the loss of U/V system

The evolution of the XX/XY system in F*. serratus* is associated with a transition towards a fully diploid life cycle in Fucales[14,40]. The transition from a U/V towards a diploid sexual system likely involved a stage of epigenetic sex determination[2,40], implying that the XX/XY system of the Fucales is fairly young compared to the 180-million-year-old Y chromosome in mammals or the 140-million-year-old W chromosome in birds[63]. A small and undifferentiated Y-specific region could explain our inability to detect the sex chromosome in *F. serratus*. We were nonetheless able to find all the ancestral V-SDR genes in the sex-homolog of *Fucus*, and several of these genes displayed a male-biased gene expression across several Fucales species, particularly *HMG-sex* that acts as the master male-sex determining factor in the U/V system. Our results indicate that *HMG-sex* and possibly other ancestral V-SDR genes are still involved in the male differentiation pathway, but likely changed their position downwards into the sex differentiation cascade. These results therefore support and extend the "bottom-up" hypothesis of sex determination, where downstream components of sex differentiation are evolutionarily conserved between taxa, and where master-sex determining genes can be pushed downwards in the cascade and be replaced by new master regulators[64].

Monoicous brown algae were previously reported to display a transcriptomic profile that is closer to that of ancestral females[26]. However, our results clearly show that co-sexuality in *C. linearis* and *D. dudresnayi* arose from a male ancestor with acquired female genes. It is likely that the female developmental program is more pleiotropic, where the expression of male-biased genes tends to be tissue-specific while female-biased genes

tend to be broadly expressed[65]. This might explain the similarity of the transcriptional profiles between females and hermaphrodites in the brown algae. The male developmental pathway may require more elements from the V-SDR for its proper activation, such as the master determinant factor *HMG-sex*[20,66] (Luthringer et al., in review), which would explain the convergent transition to monoicy from a male background. Importantly, we identified a female gene that is consistently present in both monoicous species, as well as in the U-SDR of *Ectocarpus* and *Desmarestia*, suggesting that this gene may be relevant for the determination of the female developmental pattern in the brown algae.

Hypothetical model for the evolution of haploid sex chromosomes

Here, we reconstructed the evolutionary history of the brown algal U/V system and formulate a hypothetical model for the evolution of haploid sex chromosomes (**Figure 6**). The U/V chromosomes of the brown algae descend from an ancestral autosome that contained *HMG-sex* and other important genes that would later represent the ancestral SDR. This region underwent an inversion event that initiated the differentiation of the SDR between the U and V chromosomes. The SDR subsequently expanded through the accumulation of TEs and nested inversions in each algal lineage, engulfing genes that were previously contained in the PARs. The increase in size of the SDR was further caused by acquisition of genes from autosomes. It is possible that these autosomal genes were under sexual antagonistic selection and conflict would be solved by full sex linkage of these loci. Expansions of the SDR were, accordingly, correlated with increased sexual dimorphism as each brown algal lineage evolved. Genes relevant for sex were retained within the SDR. It is possible that the continuous expansion of TEs was limited by heterochromatinization in the sex chromosome by recruiting repressive chromatin marks, which would indirectly decrease the levels of DNA repair in the sex chromosome and lead to the emergence of young TRGs that would accumulate through generation-antagonistic selection. The demise of the U/V sex chromosomes occurs in species that switch towards XX/XY or to monoicy. In the derived XX/XY system, the conserved sex-determining gene from the ancestral V sex chromosome is no longer the master male-determinant, and has moved down the sex-determination hierarchy. Transition to co-sexuality (monoicy) arose via introgression of female SDR genes in a haploid male genetic background. Finally, the demise of the U/V sex chromosomes is accompanied by a gradual loss of the genomic and evolutionary footprints of the sex chromosome, such as the accumulation of TEs and the enrichment of young TRGs, raising the possibility that recombination resumes in these genomic regions.

ACKNOWLEDGEMENTS

This work was supported by the MPG, , the CNRS, Sorbonne University, the ERC (grant n. 864038 and 638240 to SMC), the France Génomique National infrastructure project Phaeoexplorer (ANR-10-INBS-09), the JSPS Overseas Research Fellowships (to MH), the BMBF-funded de.NBI Cloud within the German Network for Bioinformatics Infrastructure (de.NBI) (031A532B, 031A533A, 031A533B, 031A534A, 031A535A, 031A537A, 031A537B, 031A537C, 031A537D, 031A538A), the Investissements d'Avenir project Idealg (ANR-10-BTBR-04-01), the European BG-01 BlueGrowth H2020 project Genialg (727892) and the ANR project Epicycle (ANR-19-CE20-0028-01). SMC is supported by the Moore Foundation (GBMF11489) and the Bettencourt-Schuller Foundation. JBR is supported by a Humboldt Research Fellowship for postdoctoral researchers from the Alexander von Humboldt Foundation. We thank the members of the Phaeoexplorer consortium, in particular

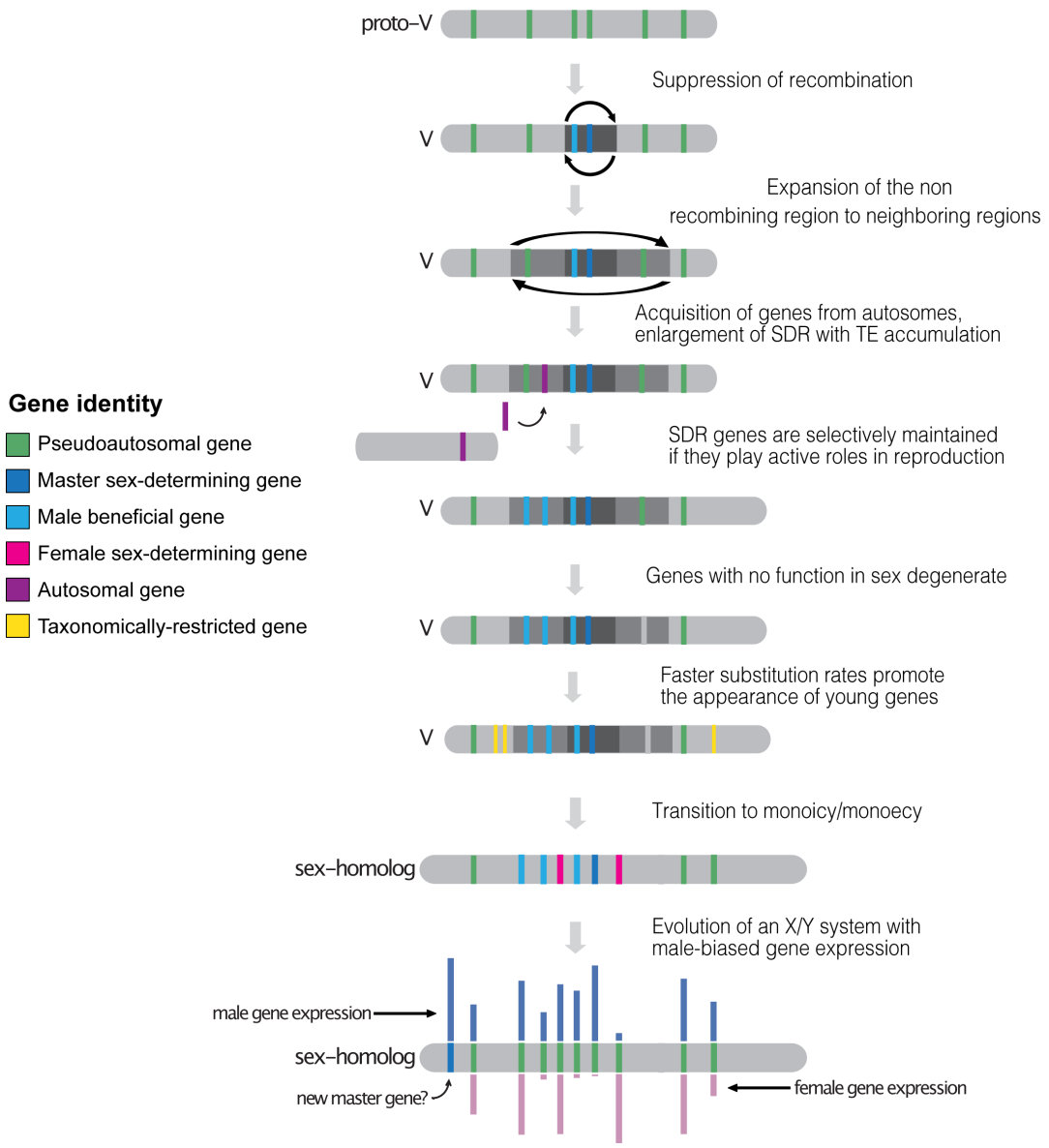

Figure 6. Hypothetical model for U/V sex chromosome evolution. U/V sex chromosomes arose from an ancestral autosome, via suppression of recombination that likely occurred via an inversion. The SDR expanded into neighboring pseudoautosomal regions (PAR) via inversions, but also by recruitment of genes from autosomes; expansion occurred in a lineage-specific fashion, concomitant with increased sexual dimorphism of the different species. SDR genes are maintained within the SDR if they have roles in sex, whereas genes with no role in sex are lost. Faster substitution rates, likely driven by the heterochromatic context of the sex chromosome may promote the rise of young genes, which are selectively maintained on the sex chromosome if they have advantages to the sporophyte generation. In species that switch to a diploid life cycle, the U/V system disappears, but the genes that are in the V-specific region retain roles in sex, although they are no longer masters. Transition from U/V separate sexes to co-sexuality (hermaphroditism) occurred when a male haploid individual acquired female-specific genes via ectopic recombination. During the demise of the U/V sex chromosomes, their structural and evolutionary footprints slowly erase.

Chloe Jolivet, Leticia Mest and Delphine Scornet for assistance with algae cultures, Corinne Cruaud for help with sequencing libraries preparation, Erwan Corre and Arthur Le Bars for support with the Phaeoexplorer database and Arnaud Couloux for the genome assemblies and annotations. We are grateful to the Roscoff Bioinformatics platform ABiMS (http://abims.sb-roscoff.fr), part of the Institut Français de Bioinformatique (ANR-11-INBS-0013) and BioGenouest network, for providing computing and storage resources.

CONTRIBUTIONS

JBR, APL: Investigation (equal); Formal analysis (equal); Methodology (equal); Visualization (equal), Writing – original draft (equal)

PL: Investigation (supporting); Formal analysis (supporting)

ED, GC, OG, KB, MH, KA, GL, EA, DL, RL, OG, SH, ZN, LG, AFP: Investigation (supporting)

GH, JMA, GP, PW, FD, JMC: Data curation (supporting); Data acquisition (supporting)

FBH: Investigation (supporting); Methodology (equal); Data curation (equal); Formal analysis (supporting)

SMC: Conceptualization (lead); Funding acquisition (lead); Methodology (equal); Project administration (lead); Supervision (lead); Visualization (supporting); Writing – original draft (equal); Writing – review and editing (lead).

SUPPLEMENTAL FIGURES

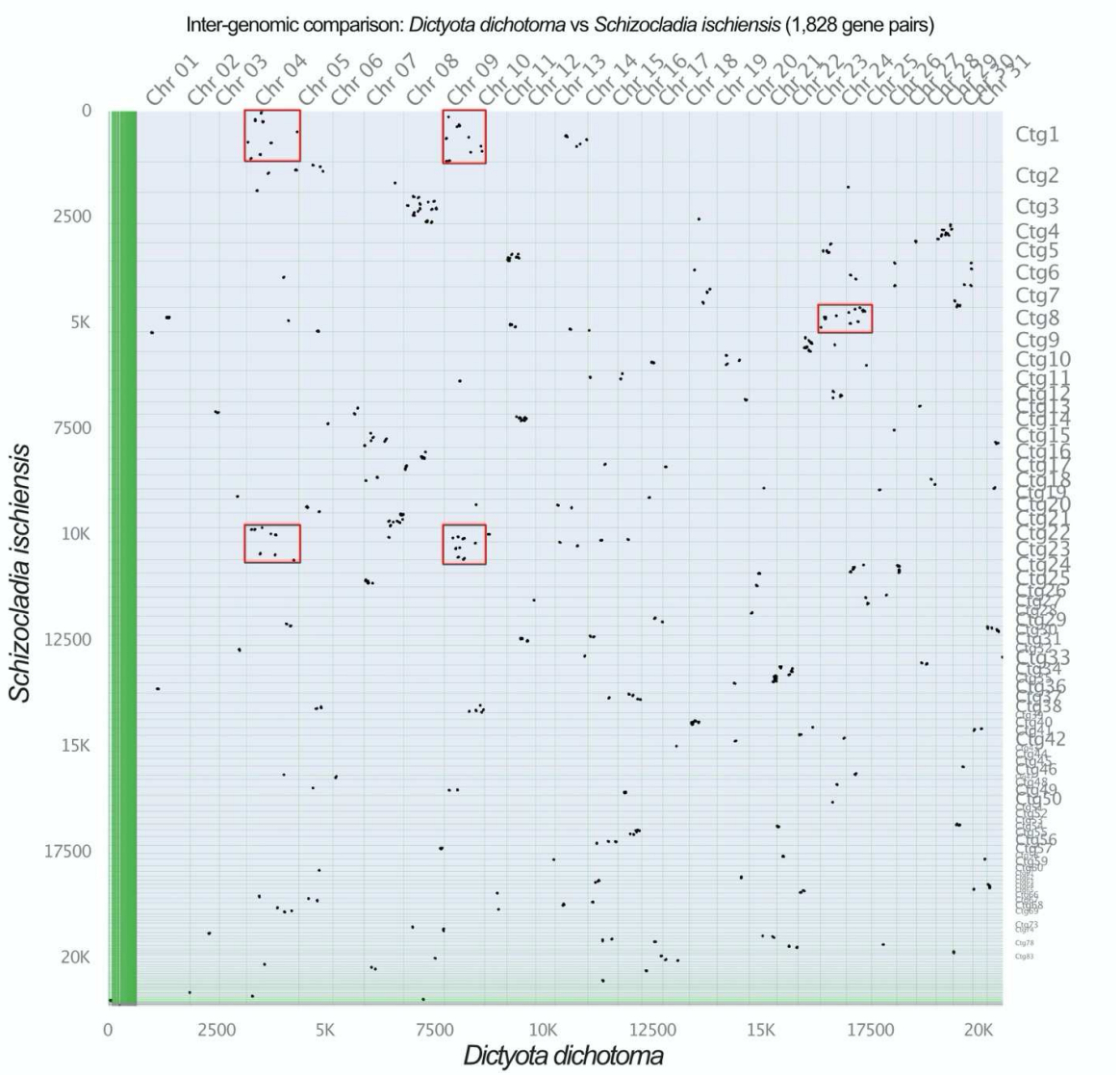

Figure S1. Macrosynteny plot between *S. ischiensis* and *D. dichotoma* using 1,828 orthologs. We highlight two fusion-with-mixing events (red squares) between chromosomes 4 and 9, and between chromosomes 23 and 24 in *D. dichotoma*.

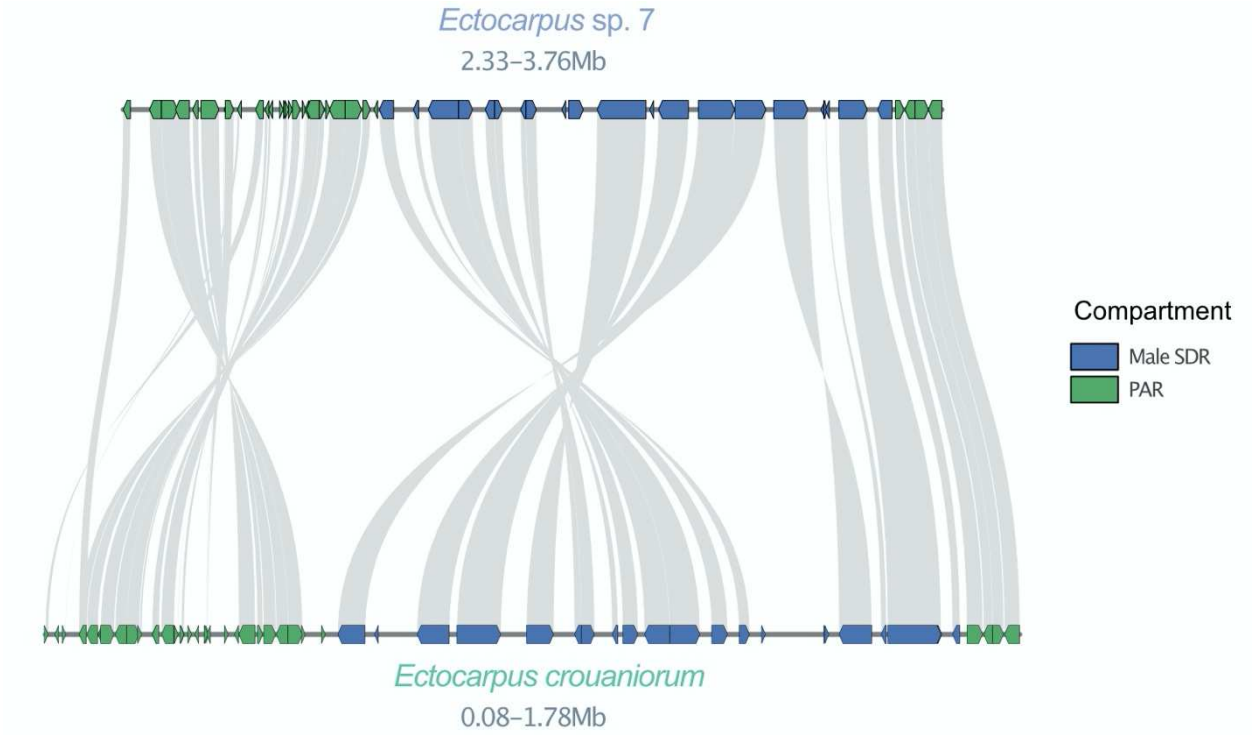

Figure S2. Male SDR synteny between *Ectocarpus* sp. 7 and *Ectocarpus crouaniorum*. Note the recent inversion event within the SDR. The arrows in the boxes represent the orientation of each gene within the chromosome.

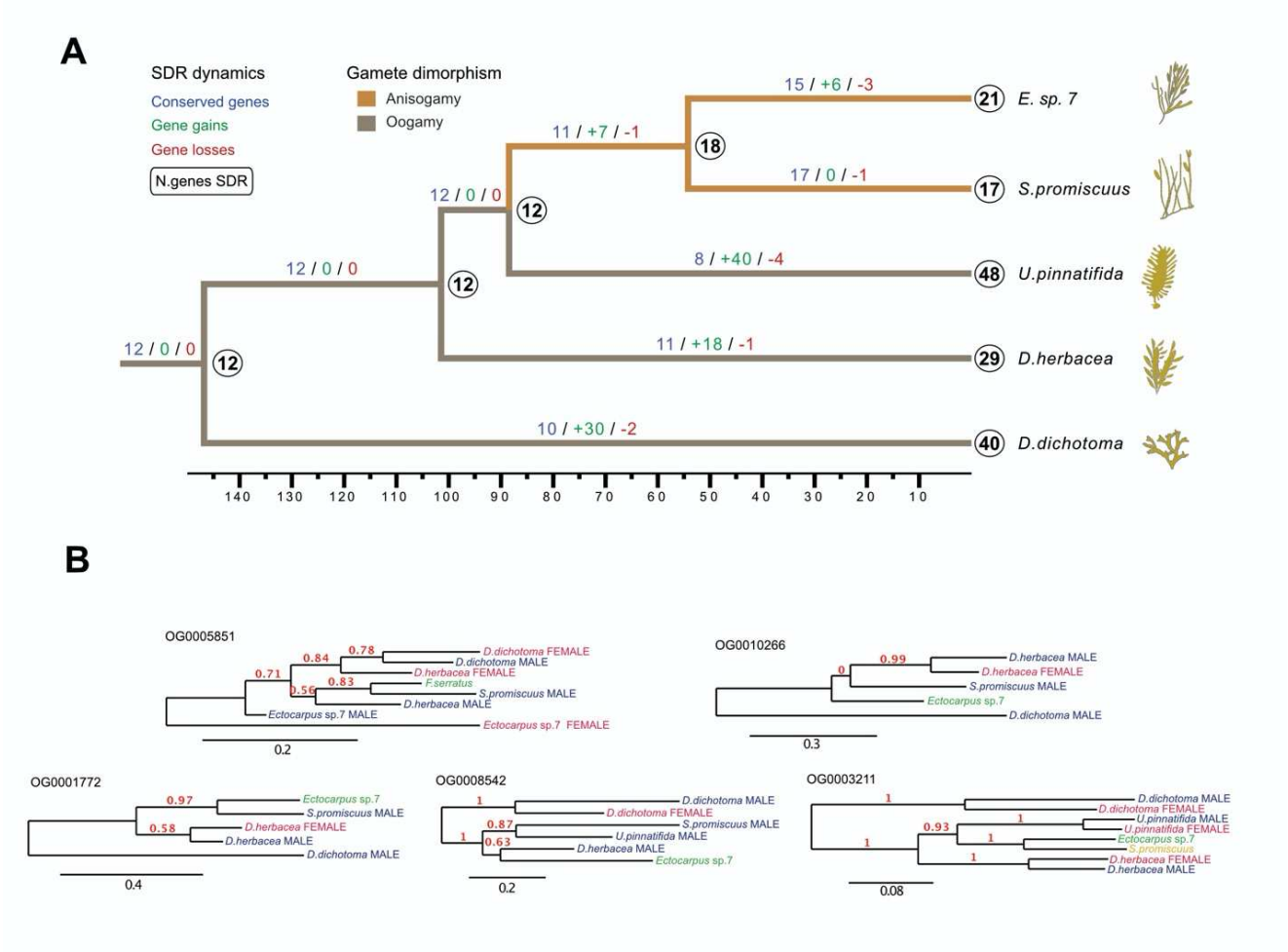

Figure S3. Detection of independently-acquired V-SDR genes across species. (A) Ancestral state reconstruction of the male SDR before accounting for independent gene acquisition. (B) Gene trees showing the independent acquisition of SDR gametologs across species that were previously interpreted as part of the ancestral male SDR genes.

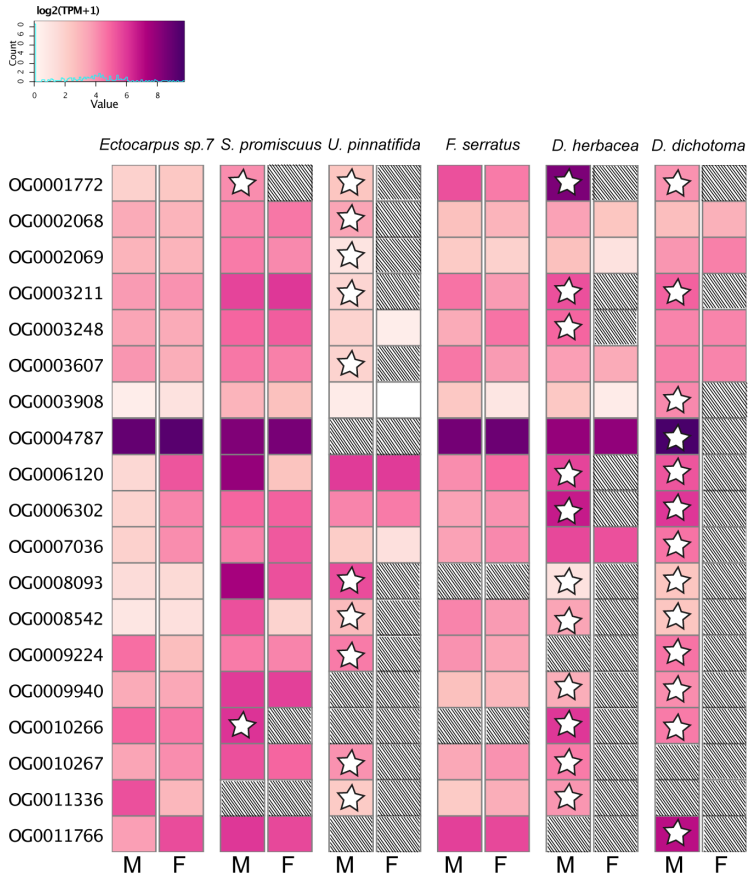

Figure S4. Expression of genes (log2(TPM+1)) that entered the SDR independently in different species. Expression is measured in mature male and female gametophytes, hashing marks missing orthologs, stars inside the cells indicate that the gene is inside the male non-recombining region (V-SDR). Orthogroups containing orthologs in less than three species or with multicopy genes were excluded from this analysis. M: male; F: female.

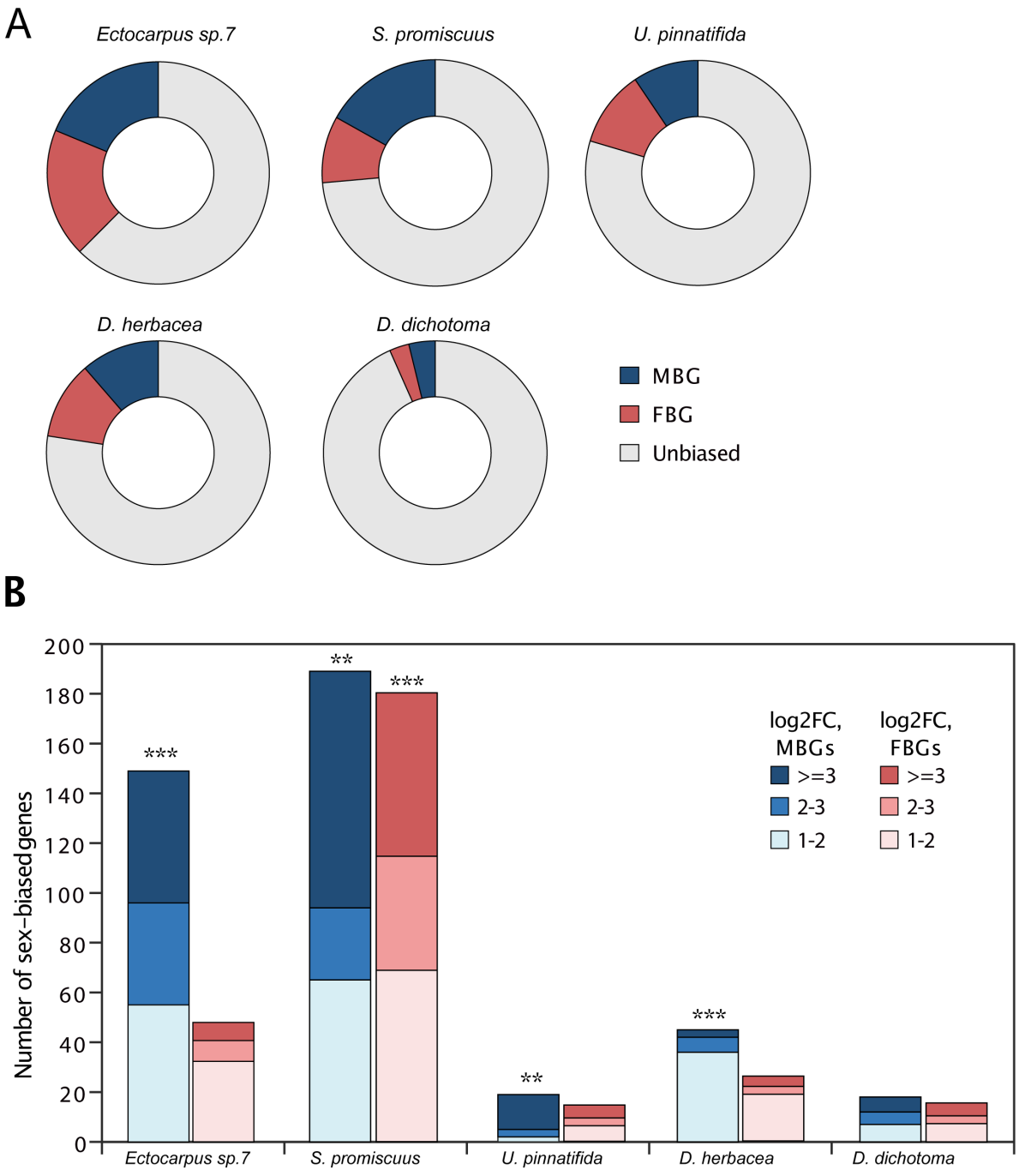

Figure S5. Sex-biased gene expression per dioicous species. (A) Proportion of sex biased genes in each of the five dioicous species. MBG: male-biased genes; FBG: female biased genes. (B) Number of sex-biased genes in the pseudoautosomal regions of sex chromosomes (SDR excluded), male-biased genes are shown in blue and female-biased genes in red. Stars above the bars mark significant enrichment of the sex-biased genes on the PAR (Chi-square test, **p<0.01, ***p<0.001).

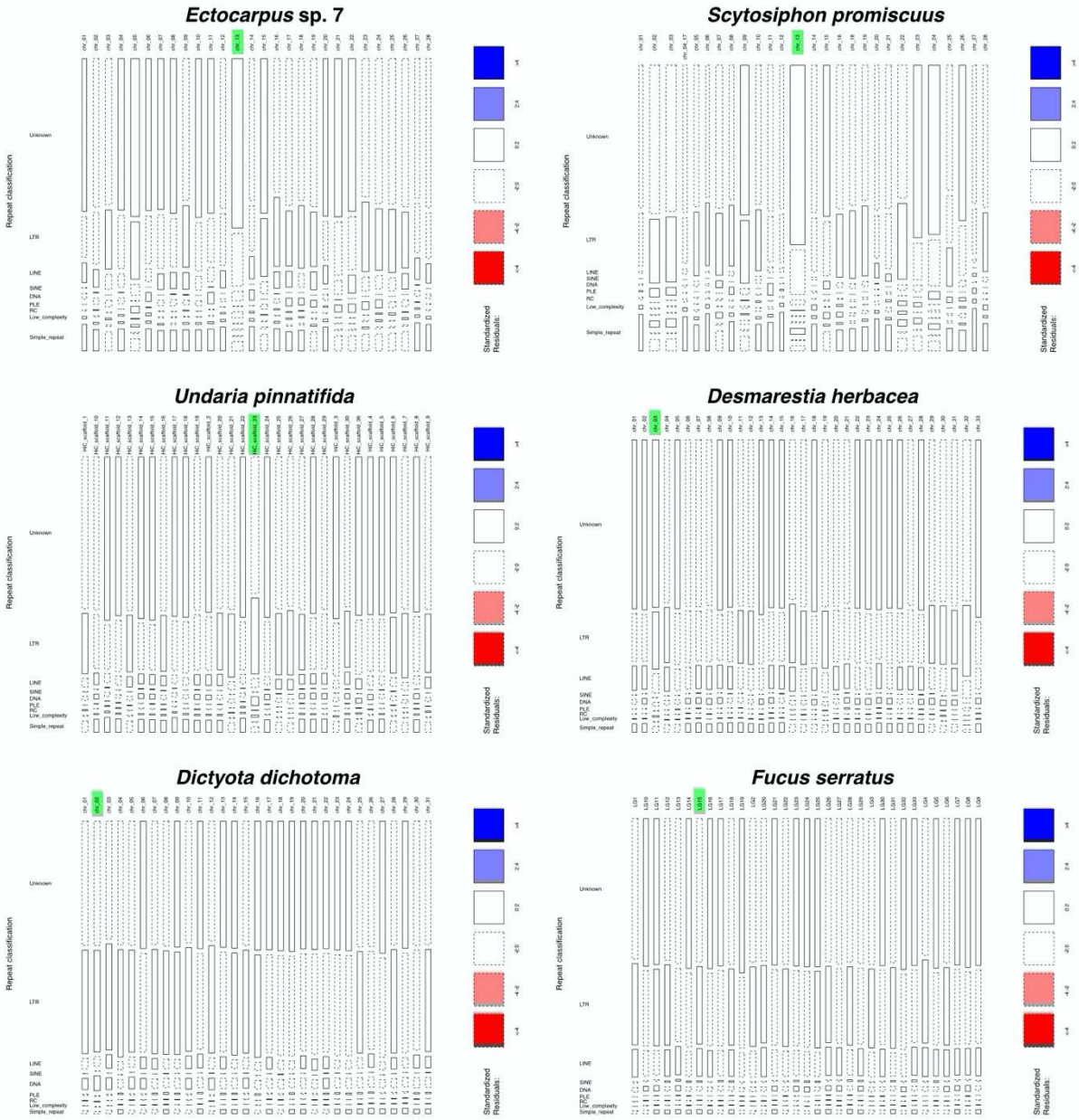

Figure S6. Distribution and proportion of classified transposable elements across the chromosomes of six brown algal species. The sex chromosome or sex-homolog is highlighted in green. The residuals in the sex chromosome were used to interpret the enrichment or depletion of Unclassified (Unknown) repetitive elements for each species.

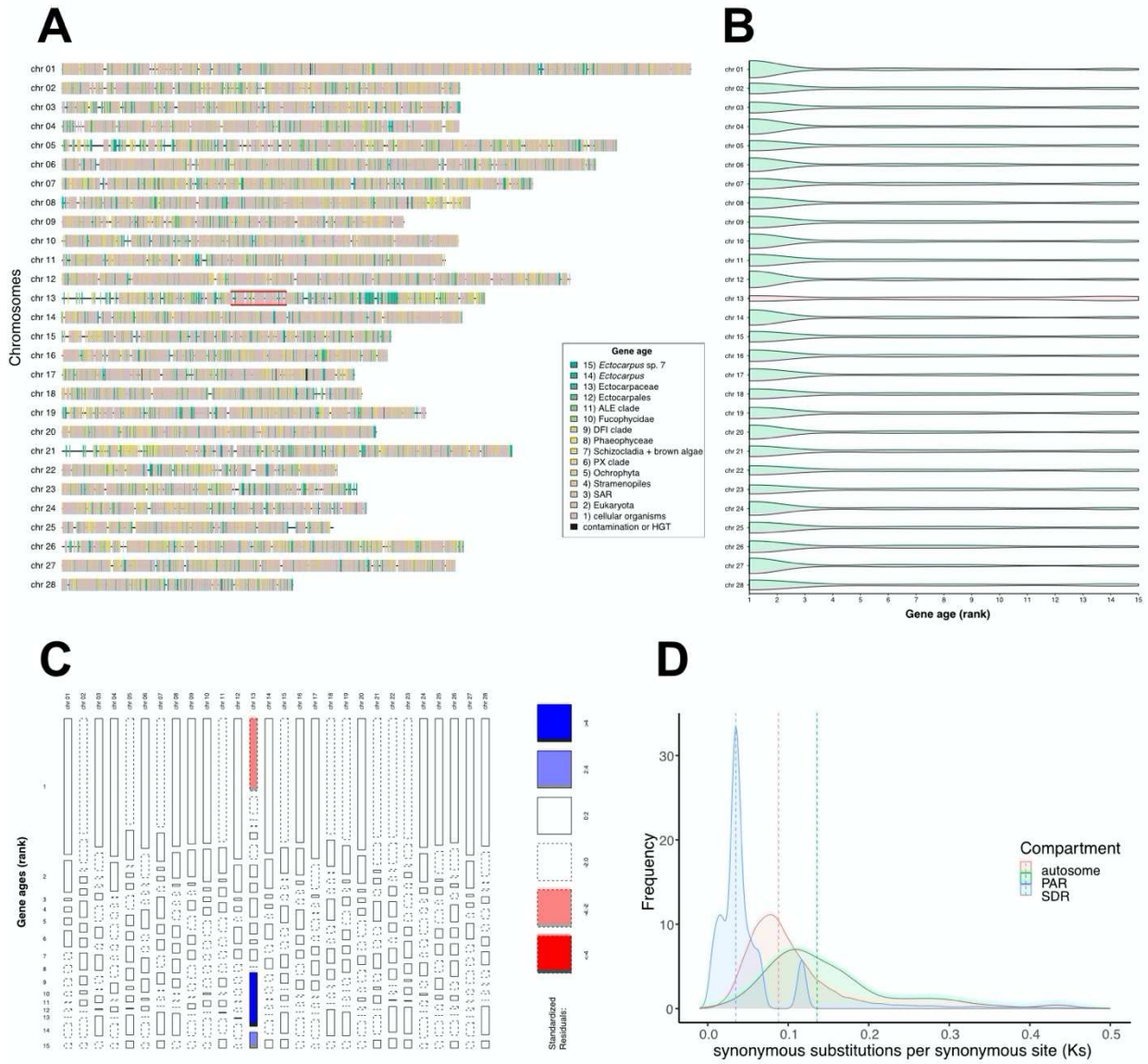

Figure S7. Gene ages across the *Ectocarpus* sp.7 genome. (A) Distribution of relative gene ages across the chromosomes of *Ectocarpus* sp. 7. The SDR of the sex chromosome (chr 13) is highlighted with a red box. (B) The sex chromosome (red) has a significantly higher proportion of young genes and a lower proportion of old genes when compared to the autosomes (green; see Table S11). (C) Mosaic plot showing that the species-level (rank 15) and the genus-level (rank 14) genes are responsible for the enrichment of young genes in the sex chromosome. (D) The *Ks* values are significantly higher in the PARs of the sex chromosome when compared to the autosomes or the SDR (see Table S13).

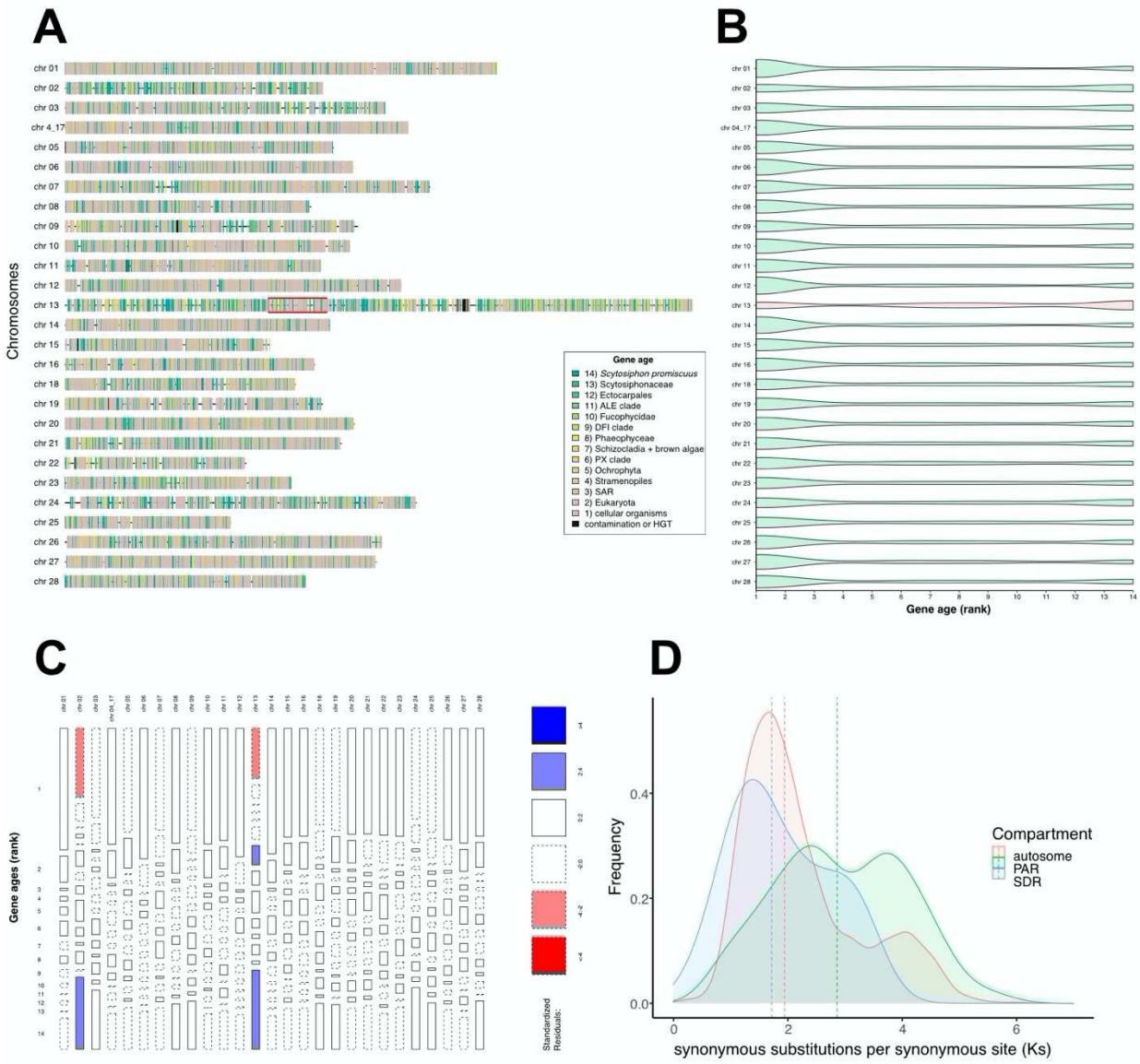

Figure S8. Gene ages across the *S. promiscuus* genome. A) Distribution of relative gene ages across the chromosomes of *Scytosiphon promiscuus*. The SDR of the sex chromosome (chr 13) is highlighted with a red box. (B) The sex chromosome (red) has a significantly higher proportion of young genes and a lower proportion of old genes when compared to most of the autosomes (green; see Table S11). (C) Mosaic plot showing that the species-level (rank 14) genes are responsible for the enrichment of young genes in the sex chromosome. (D) The *Ks* values are significantly higher in the PARs of the sex chromosome when compared to the autosomes or the SDR (see Table S13).

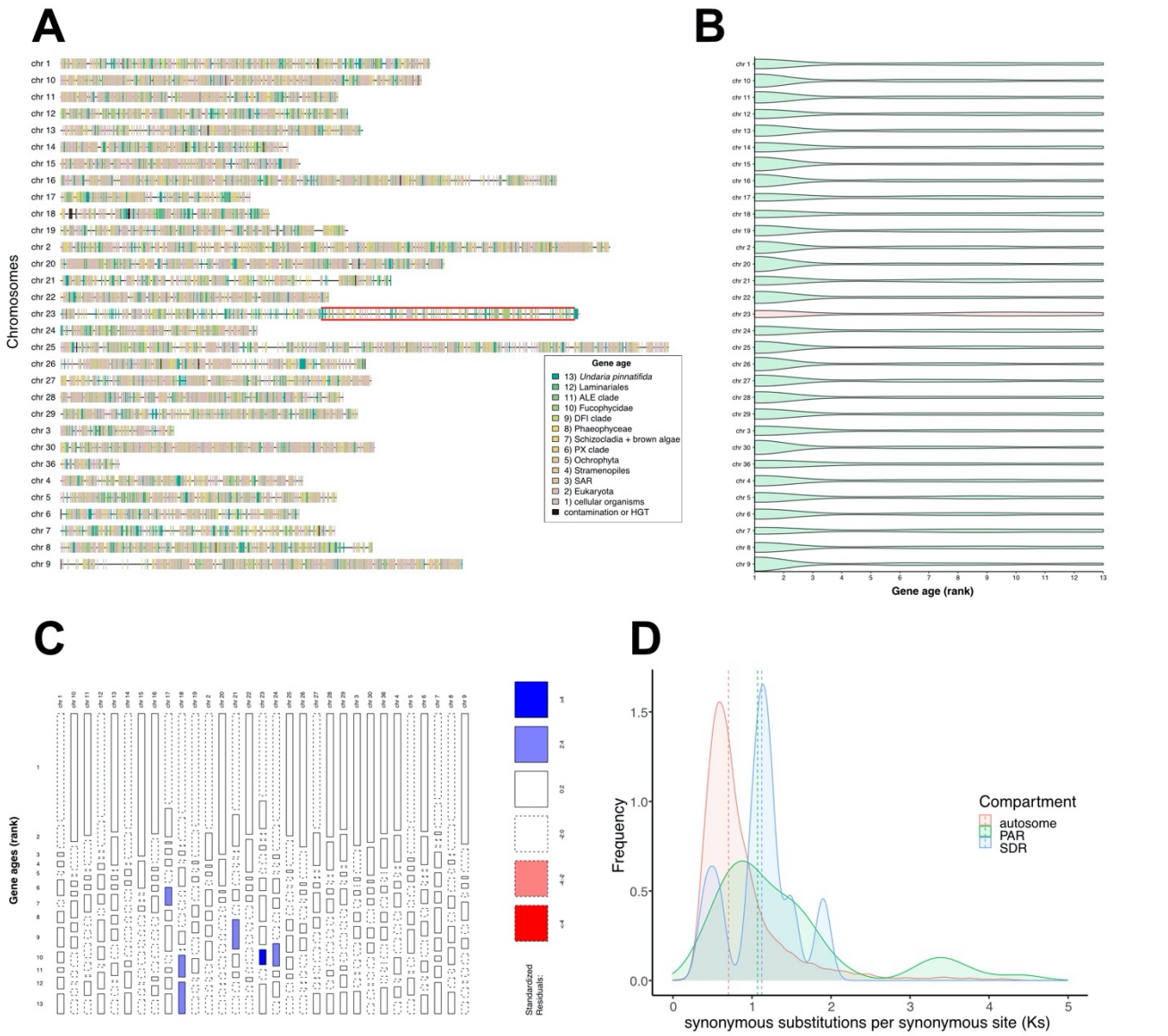

Figure S9. Gene ages across the *U. pinnatifida* genome. (A) Distribution of relative gene ages across the chromosomes of *Undaria pinnatifida*. The SDR of the sex chromosome (chr 23) is highlighted with a red box. (B) The sex chromosome (red) has a significantly higher proportion of young genes and a lower proportion of old genes when compared to most of the autosomes (green; see Table S11). (C) Mosaic plot showing that the ALE-clade genes (rank 11) are responsible for the enrichment of young genes in the sex chromosome. (D) The *Ks* values are significantly higher in the sex chromosome when compared to the autosomes (see Table S13), showing similar values in the PARs and in the SDR.

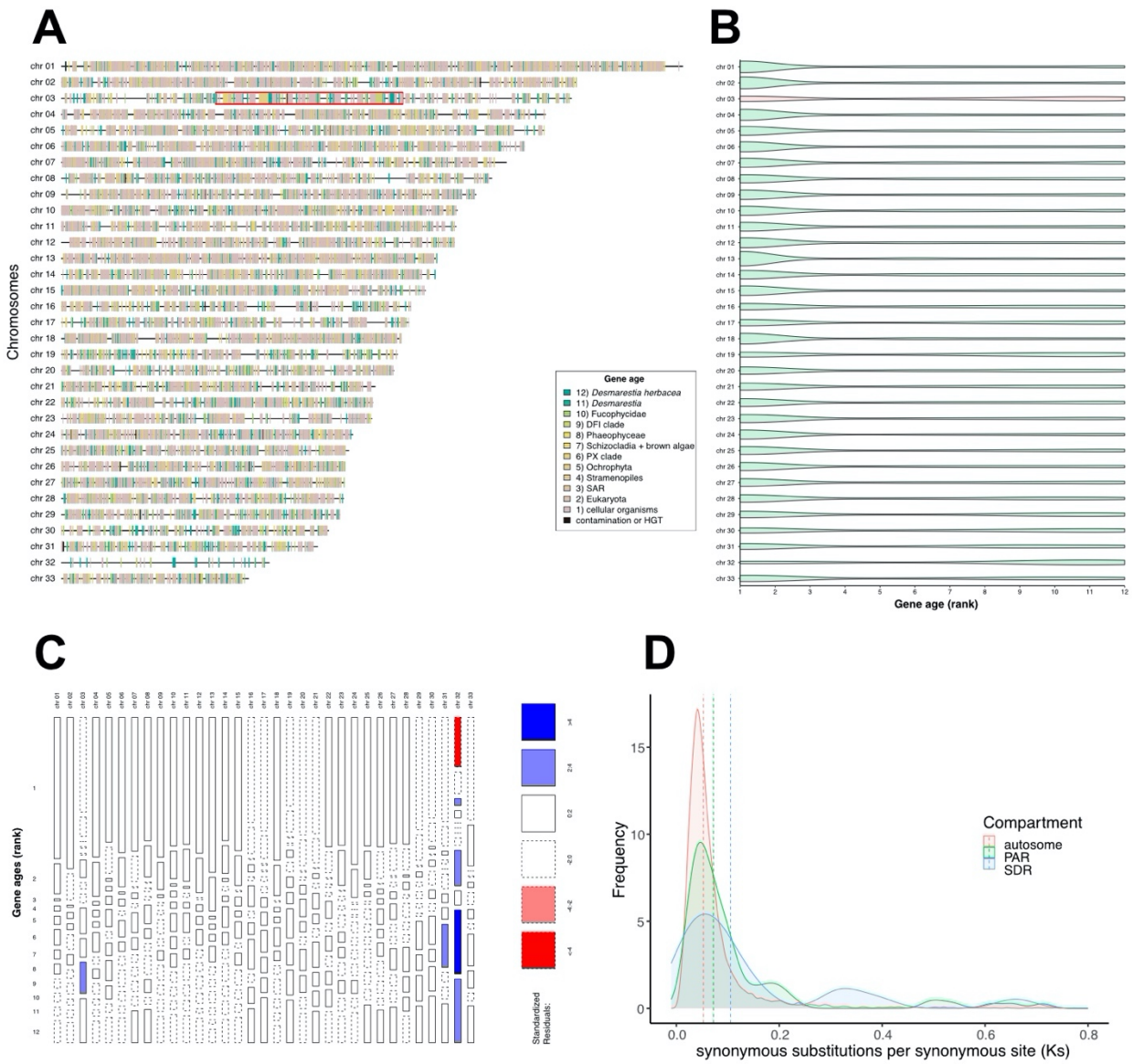

Figure S10. Gene ages across the *D. herbacea* genome. (A) Distribution of relative gene ages across the chromosomes of *Desmarestia herbacea*. The SDR of the sex chromosome (chr 03) is highlighted with a red box. (B) The sex chromosome (red) has a significantly higher proportion of young genes and a lower proportion of old genes when compared to most of the autosomes (green; see Table S11). (C) Mosaic plot showing that the genus-level (rank 11) genes are responsible for the enrichment of young genes in the sex chromosome. (D) The *Ks* values are significantly higher in the sex chromosome when compared to half of the autosomes (see Table S13). Non-significance of *Ks* values across chromosomes may be driven by the conflation with the *Ks* values in *Desmarestia dudresnayi*. The SDR displays higher *Ks* values compared to the PARs or the autosomes.

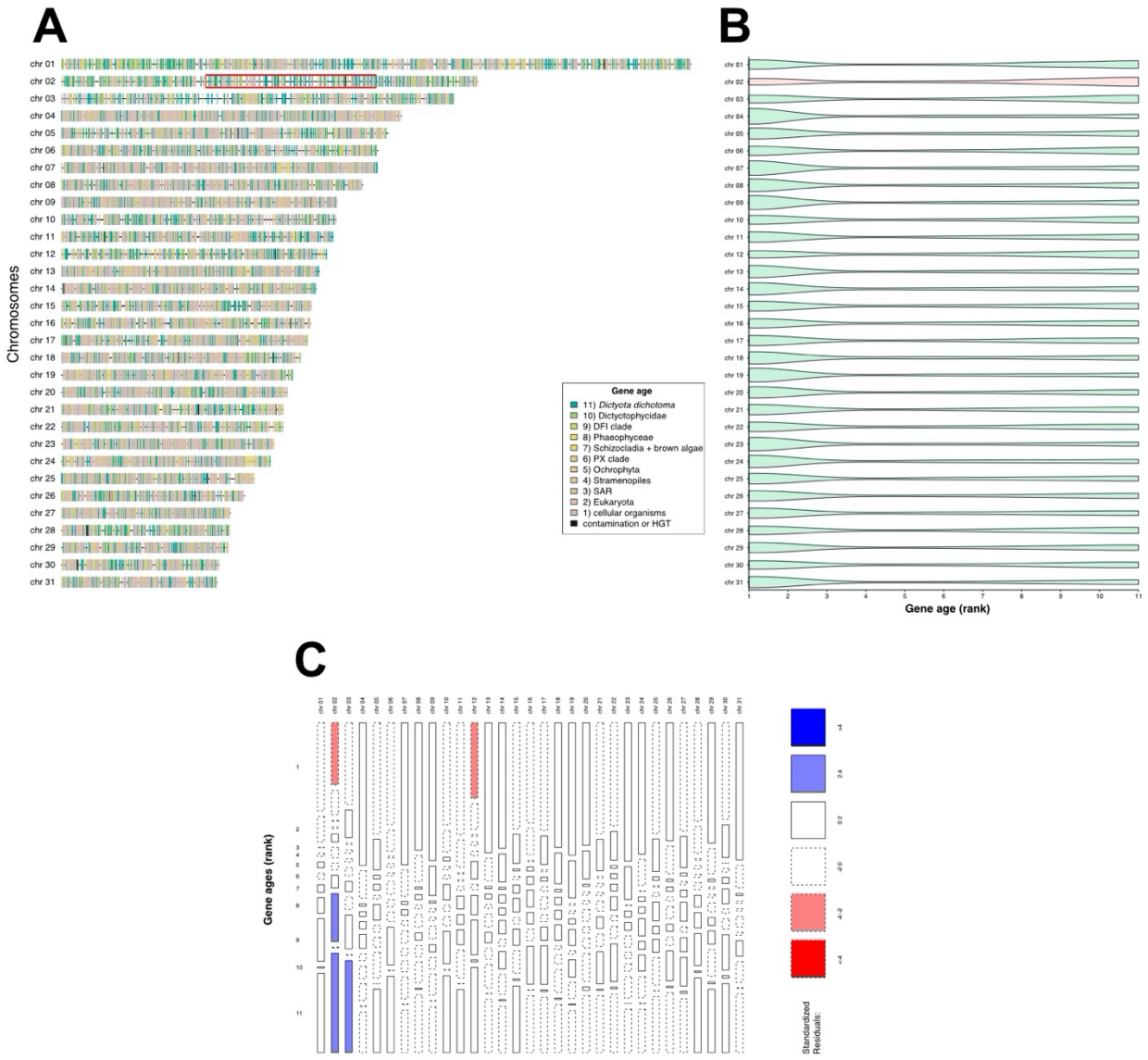

Figure S11. Gene ages across the *D. dichotoma* genome. (A) Distribution of relative gene ages across the chromosomes of *Dictyota dichotoma*. The SDR of the sex chromosome (chr 02) is highlighted with a red box. (B) The sex chromosome (red) has a significantly higher proportion of young genes and a lower proportion of old genes when compared to most of the autosomes (green; see Table S11). (C) Mosaic plot showing that the species-level (rank 11) and the DFI-clade-level (rank 9) genes are responsible for the enrichment of young genes in the sex chromosome. *Ks* values were not calculated for *D. dichotoma*, due to a saturation of synonymous mutations with the closest species in the PhaeoExplorer database (*Halopteris paniculata*).

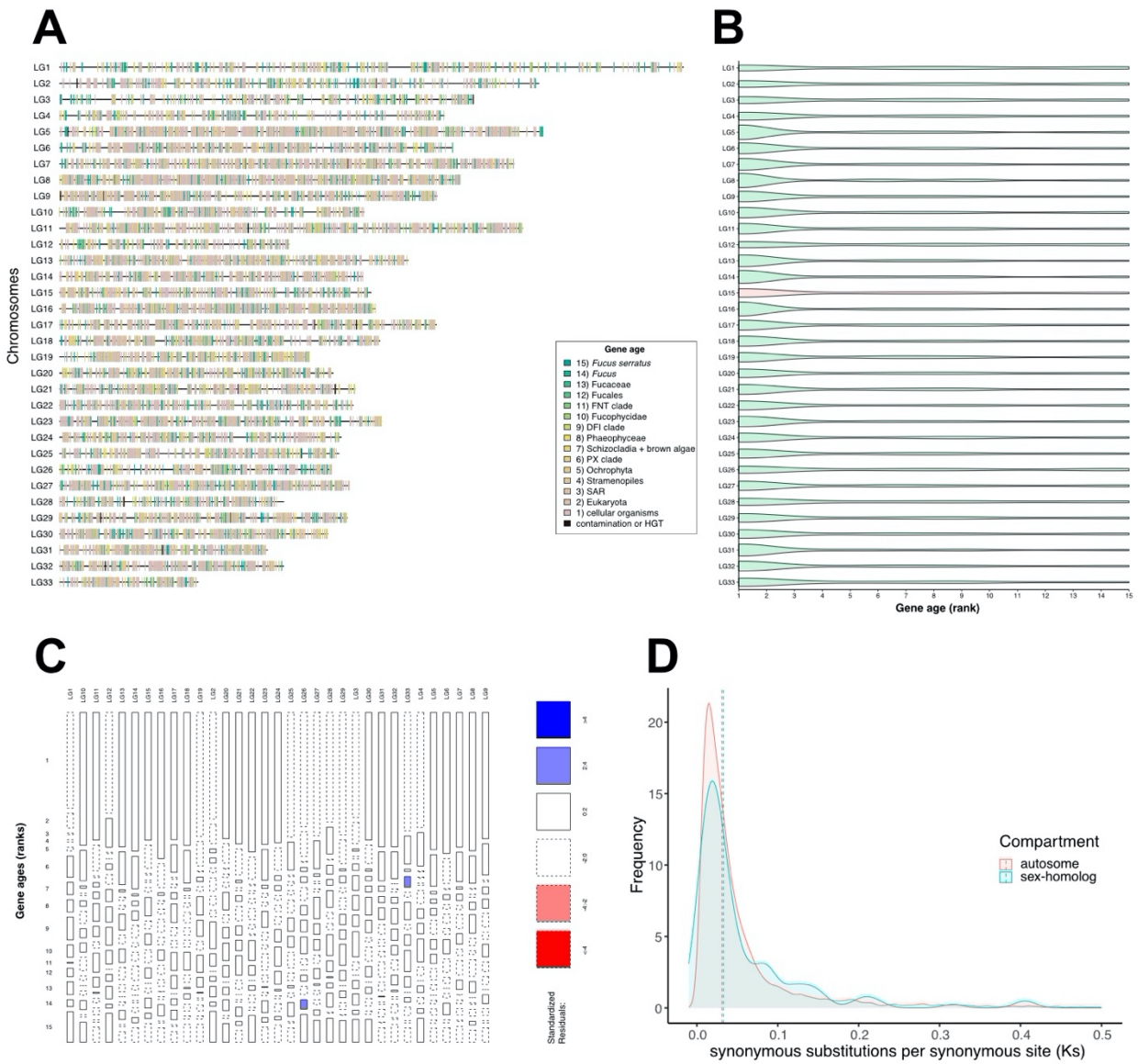

Figure S12. Gene ages across the *F. serratus* genome. (A) Distribution of relative gene ages across the chromosomes of *Fucus serratus*. (B) The sex-homolog in *F. serratus* (LG15; red) shows no significant differences in gene age distribution when compared to the rest of the chromosomes (green; see **Table S11**). (C) Mosaic plot showing no discernible pattern of gene age distribution in any of the chromosomes. (D) The *Ks* values are similar in the sex-homolog when compared to the other chromosomes (see **Table S13**).

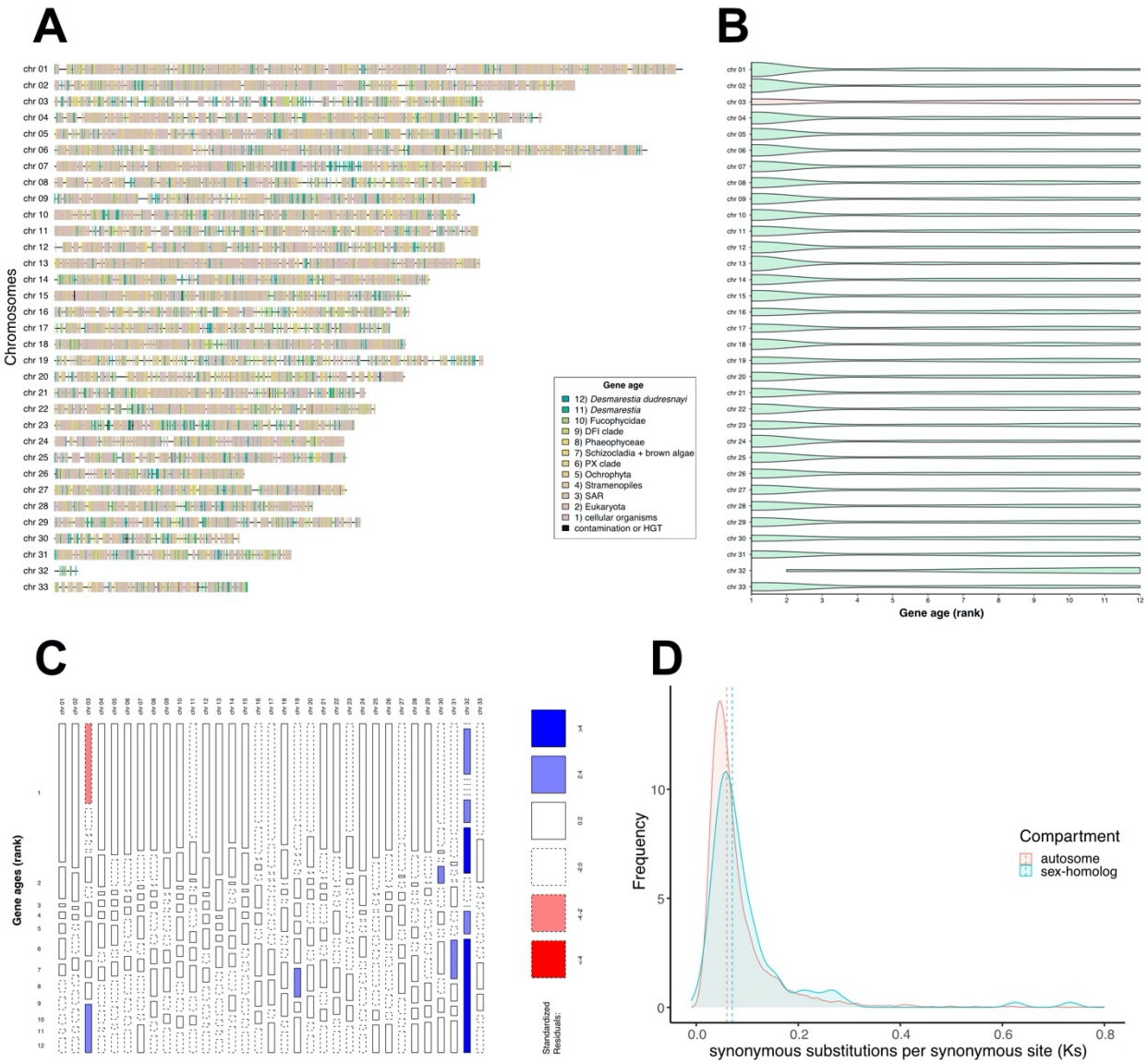

Figure S13. Gene ages across the *D. dudresnayi* genome. (A) Distribution of relative gene ages across the chromosomes of *Desmarestia dudresnayi*. (B) The sex-homolog in *D. dudresnayi* (chr 03; red) has a significantly higher proportion of young genes and a lower proportion of old genes when compared to most of the other chromosomes (green; see **Table S11**). (C) Mosaic plot showing that the species-level genes (rank 12) are responsible for the enrichment of young genes in the sex-homolog. (D) The *Ks* values are similar in the sex-homolog when compared to the other chromosomes (see **Table S13**).

METHODS

Biological material

Scytosiphon promiscuus, Dictyota dichotoma, *Undaria pinnatifida* and *Desmarestia dudresnayi* haploid gametophytes were cultivated in the laboratory conditions as in [67]. We cultivated the gametophytes at 14°C with a photoperiod of 12:12 h light:dark an irradiance of 25µmol photons.m-2.s-1. The media consisted of filtered natural seawater (NSW), which was autoclaved and enriched with half-strength Provasoli nutrient solution (Provasoli-enriched seawater; PES)[67]. We grew the first biomass in 140mm Petri dishes and the gametophytes were later transferred to 1L flask with gentle aeration. The gametophytes were fragmented once a month and the media were changed every two weeks to promote biomass production. Prior to freezing, gametophytes were treated with antibiotics for 3 days with a gentle agitation and under the same culture conditions. The first day, gametophytes were treated with a mix Streptomycin (2g/L of PES), Penicillin G (0.5g/L of PES) and Chloramphenicol (0.1g/L of PES); the next day with Ampicilin (1g/L of PES) and finally the last day with Kanamycin (1g/L of PES). Between each day of treatment and before freezing, gametophytes were rinsed with 500mL of NSW to remove the traces of antibiotic.

Samples for fucoid algae sexual and vegetative tissue were collected in the intertidal zone during low tides in June 2012 from Viana do Castelo (*F. vesiculosus*, *A. nodosum*) and Caminha (Rio Minho; *F. ceranoides*), northern Portugal. Sexual phenotypes were verified in the field by sectioning and observing receptacles under a field microscope. Tissue samples were flash-frozen in liquid nitrogen on the shore and transported to the laboratory in a cryoshipper, after which they were lyophilized and stored dry at room temperature on silica crystals. See **Table S22** for list of strains used in this study.

DNA and RNA extraction and sequencing

Genomic DNA was isolated from algal tissue (~100mg) by grinding into fine powder under liquid nitrogen and subsequent cell lysis in 500µL of Genomic Lysis Buffer (OMNIPREP for plant kit) for 1 hour at 60°C. The lysate was cleaned up with 200µL of chloroform and DNA was precipitated in EtOH. The DNA pellet was digested in CF buffer (Macherey-Nagel) for 45 min at 65°C and purified using NucleoBond AXG20 Mini columns according to the user manual (Macherey-Nagel). Final high molecular weight gDNA was quantified (Qubit), analyzed for purity (Nanodrop) and checked for size distribution (Femto Pulse System) before preparing the sequencing libraries. We sequenced the libraries using an Oxford Nanopore Technologies (ONT) MinION Mk1B. We prepared the ONT libraries using an SQK-LSK110 library preparation kit for R9.4.1 flow cells and an SQK-LSK114 library preparation kit for R10.4.1 flow cells. Two libraries were sequenced for *Desmarestia dudresnayi* on R9.4.1 flowcells and a third library was sequenced on a R10.4.1 flowcell.

RNA was isolated from mature gametophytes of *Undaria pinnatifida* and *Scytosiphon promiscuus* following modified procedure of Qiagen RNAeasy kit26 and the TruSeq RNA Library Prep Kit v2 was used to sequence the transcriptomes in an Illumina NextSeq 2000 platform (150bp, PE reads). Extraction of total RNA from fucoid algae (*F. vesiculosus, A. nodosum* and *F. ceranoides*) was performed following 65 and RNA libraries were sequenced on Illumina HiSeq 2000 machine (100 bp, PE reads).

Genome assembly and annotation

Whole-genome assemblies and annotations of *S. promiscuus* male, *D. dichotoma* male, *D. herbacea* male and female, *E. crouanorium* male, *C. linearis*, *S. ischiensis* and *F. serratus* male were obtained from Denoeud et al, (submitted). We also downloaded the male genomes of *Ectocarpus* sp. 7[68] and *Undaria pinnatifida*[69] which were already assembled at a chromosome level. For *Desmarestia dudresnayi*, we performed a *de novo* genome sequencing and annotation. Base calling was done using ONT Guppy[70] with the configuration files dna_r9.4.1_450bps_sup.cfg and dna_r10.4.1_e8.2_400bps_sup.cfg and the options --trim_adapters –trim_primers, yielding 17.4 Gbp of data in 2,871,152 reads. We merged all the reads and analyzed them using Kraken v2.1.2[71] and the bacteria database (downloaded 08-2022) to remove potential contaminant sequences. All data classified as bacterial reads by Kraken were screened using blastN v2.13.0+[72] (-evalue 0.001 -num_alignments 20) against the NCBI genbank bacterial database (downloaded 11-2023). The blastN output was visualized in MEGAN v6.23.4[73], and all the reads that were declared as bacterial were extracted and removed from further analyses. We obtained 1,908,772 decontaminated reads with an average length of 5.1Kbp (9.8 Gbp of data, 20x coverage), which were deposited on the NCBI Sequence Read Archive (see **Table S22**).

The decontaminated reads were assembled *de novo* using flye v2.9.1-b1780[74] with the options '--nano-raw -g 450m -t 28 -i 3 --scaffold'. The draft assembly consisted of 1,032 contigs with a total size of 425 Mbp, an N50 of 4.6 Mbp and an L50 of 29 contigs. We used TransposonPSI (http://transposonpsi.sourceforge.net/) to predict the transposable elements and RepeatScout[75] to predict the simple repeats in the genome assembly. Both predictions were combined to soft-mask the repetitive content in the genome assembly using bedtools maskfasta[76]. We mapped the RNA-seq data of *Desmarestia dudresnayi* from the PhaeoExplorer database (Deneoud et al, submitted) to the soft-masked genome assembly using STAR[77]. We used BRAKER alongside the RNA-seq data[78] to predict the protein-coding genes in the soft-masked genome assembly.

Hi-C library preparation and sequencing for chromosome-level assemblies

We generated Hi-C libraries for three male genomes (*Scytosiphon promiscuus*, *Desmarestia herbacea* and *Dictyota dichotoma*) and two female genomes (*Ectocarpus* sp. 7 and *Desmarestia herbacea*). Fresh algal tissue was cross-linked for 20 minutes at room temperature in a solution of 2% formaldehyde with filtered natural sea water (NSW) and then transferred into a 400 mM Glycine solution with filtered NSW for five minutes to quench the formaldehyde. The samples were then stored at -80°C until use. The Hi-C libraries were prepared as follows. The samples were de-frosted in 1 mL of 1x *Dpn*II buffer with protease inhibitors (Roche cOmplete™), transferred to Precellys VK05 lysis tubes (Bertin Technologies, Rockville, MD) and disrupted using the Precellys apparatus with five grinding cycles of 30 seconds at 7,800 rpm followed by 20 second pauses. SDS was added to the lysate at 0.5% final concentration and samples were incubated for 10 minutes at 62°C, followed by the addition of Triton-X100 to a final concentration of 1% and 10 minutes of incubation at 37°C under gentle shaking. We added 500 U of *Dpn*II to 4.6 mL of the digestion mixture and incubated the samples for two hours at 37°C under gentle shaking (180 rpm in an inclined rack to prevent sedimentation), followed by the addition of another 500 U of *Dpn*II and an overnight incubation under the same conditions. The digested samples were centrifuged at 4°C for 20 minutes at 16,000×g. The supernatant was discarded and the pellet was incubated for biotinylation at 37°C for an hour under a constant shaking (300 rpm) in a 500 ml biotinylation mix with a concentration of 1x ligation buffer, 0.09 mM of dATP-dGTP-dTTP, 0.03 mM of Biotin-14-dCTP and

0.64 U/mL of Klenow fragments. After biotinylation, the samples were incubated for three hours at room temperature in a 1.2 mL ligation reaction with a concentration of 1x ligation buffer, 100 mg/mL of BSA, 1 mM of ATP and 0.4 U/mL of T4 DNA Ligase. The samples were then incubated overnight at 65°C after adding 20µl of 0.5M EDTA, 80µl of 10% SDS and 1.6 mg of Proteinase K. DNA was extracted with 1 volume of phenol/cholorform/isoamyl (24:24:1) alcohol, followed by 30 seconds of vortex at top speed and a five-minute centrifugation at top speed. We precipitated the DNA by adding 1/10 volume of 3M NaAC pH5 and two volumes of cold EtOH 100%, followed by a 30-minute incubation at -80°C and a 20-minute centrifugation at 14,000×g and 4°C. The DNA pellet was washed with 1mL of EtOH 70%, then dried at 37°C for 10 minutes and resuspended in 100µl 1x TE buffer with 1mg/ml of RNase. DNA was sheared to 250-500bp fragments using Covaris S220, purified with AMPure beads (0.6X) (Beckman) and eluted in 20µl 10mM Tris pH8.0. Biotinylated but not ligated DNA fragments were first removed by T4 DNA polymerase treatment (final concentration=300 U/pellet; NEB), and the biotin-labeled fragments were selectively captured by Dynabeads MyOne Streptavidin C1 (Invitrogen). The libraries were prepared using NEB Ultra II library preparation system and sequenced on the NextSeq2000 Illumina platform (2x150 bp) (**Table S22**).

We scaffolded the genomes from Denoeud et al, (submitted) into chromosome-level assemblies using the Hi-C data. Additionally, the female SDR of *Ectocarpus* p. 7 was previously merged into a single scaffold without knowing the correct order of the contigs[68], so we separated these contigs to reorganize them in the correct order using Hi-C data. We filtered the low-quality Hi-C reads using Trimmomatic[79] (ILLUMINACLIP:2:30:10 LEADING:25 TRAILING:25 SLIDINGWINDOW:4:15 MINLEN:75 AVGQUAL:28). We mapped the Hi-C reads against each genome assembly using BWA-mem[80] as implemented in the Juicer pipeline[81] to generate a contact map, which was then fed to 3D-DNA[82] to scaffold the genomes into chromosomes. The obtained scaffolds were manually inspected against the contact maps to solve the limits of each chromosome using Juicebox[83]. The PhaeoExplorer gene annotations (Denoeud et al, submitted) were lifted into the new assemblies using Liftoff[84], while the annotation of transposable elements was performed using RepeatModeler2[85]. We scaffolded the genomes of *Ectocarpus crouaniorum* and *Desmarestia dudresnayi* into chromosomes using a reference-guided assembly with RagTag[86] against the chromosome-level assemblies of *Ectocarpus* sp. 7 and *Desmarestia herbacea*, respectively.

Discovery of the UV sex determination regions

Male sex determining regions (V-SDR) in *S. promiscuus*, *U. pinnatifida*, *D. herbacea* and *D. dichotoma,* as well as female sex determining region (U-SDR) in *D. herbacea* were analyzed following a YGS approach developed by Carvalho and Clark[87] and coverage analysis described previously[88]. The YGS method principle is to identify male or female sex-linked scaffolds by comparing kmer frequencies between reference genome assembly and kmers generated from DNAseq reads of the opposite sex. Regions in the male reference genome with low density coverage of female kmers will indicate candidate male SDR sequences, similarly, female genomic scaffolds with low coverage in male kmers will denote female SDR region. First, fifteen base pair kmer sequences were generated from respective Illumina reads (**Table S22**) using Jellyfish count (-m 15 -s 10G -C --quality-start=33 --min-quality=20) and converted to fasta format with Jellyfish dump (--lower-count=5)[89]. Next, non-overlapping 100kb sliding windows of the reference chromosome genome assemblies were created using seqkit[90] and used as input for the YGS.pl script together with the fasta kmer files produced in the previous step. Genomic windows with a minimum of 70% of unmatched single copy kmers were then retained as

candidate male or female SDR sequences. These regions were further validated by the coverage analysis. In detail, the short Illumina reads coming from males and females of each investigated species were trimmed with Trimmomatic[79] (see above) and mapped to the reference genome, for which the SDR was to be studied, using HISAT2[91] (default settings). Bam files produced by HISAT2 were used as input for Mosdepth[92] to calculate coverage in 100kb windows along the genome sequence (-m -n -b 100000 --fast-mode -Q 30). Read mapping depth in genomic windows was normalized by the genome-wide mean for each sex and the coverage in genomic intervals was then compared between males and females. Because V-SDR-linked sequences are present only in males, we expect them to have similar read coverage as autosomal regions in males, but little or no coverage in females (and conversely for the U-SDR sequences). The comparison focused on regions within male reference genomes where the coverage in males fell within the range of 75% to 125% of the genome average, while the coverage in females remained below 50% of the genome average. These findings were then cross-referenced with the results obtained from the YGS analysis. The reverse strategy was applied to female U-SDR regions for a comprehensive evaluation. Both, coverage and kmer analysis, identified identical genomic regions (**Table S1**).

Genetic mapping and search for the sex chromosome in *Fucus serratus*

Three different sets of materials were used in this study: (i) twelve male and twelve female field samples hereafter denoted the 24-individual natural population; (ii) 157 sporophyte progeny population derived from a cross between one male sample and one female sample collected from the field and (iii) three male and three female samples collected from the field for whole-genome sequencing. The 157-progeny population and 24-individual natural population were genotyped by double digest RAD sequencing approach (ddRAD-seq). Briefly, individual genomic DNA was digested with the restricted enzymes PstI and HhaI to obtain fragments that were size selected between 400 and 800 bp before sequencing on in Illumina HiSeq 2500 platform (paired-end 2 x 125 bp). See [93] for detailed protocol of the ddRAD-seq.

We performed whole-genome sequencing on Illumina HiSeq 2500 (2x 150 bp paired-end) for the three male and three female samples. For ddRAD-seq data, raw reads were cleaned and trimmed with Trimmomatic as above and mapped to the draft genome of *Fucus serratus* male. For the progeny population, genotypes were called from the obtained bam files, using the Stacks pipeline (v2.5)[94]. The obtained vcf files were filtered with vcftools[95] and bcftools[96] (max missing per locus:30%, max missing per sample:40%, max mean coverage:30, minQG:20).

The filtered vcf file of the progeny population was used to construct a genetic map with Lep-MAP3[97]. Briefly, ParentCall2 module was used to call parental genotypes, SeparateChromosomes2 module was used to split the markers into linkage groups and OrderMarkers2 module was used to order the markers within each linkage group using 30 iterations per group and finally computing genetic distances. Phased data were converted to informative genotypes with the script map2genotypes.awk.

We used different approaches to identify the SDR in *Fucus serratus*:

Coverage analysis: We combined whole-genome sequence data from the three males and three females alongside the ddRAD-seq data of the 24-individual natural population, mapping both datasets to the *F. serratus* male genome assembly using bwa-mem[80]. Coverage analyses have been done in several ways:

- Using SATC (sex assignment through coverage)[98], a method that uses sequencing depth distribution across scaffolds to jointly identify: (i) male and female individuals, and (ii) sex-linked scaffolds. This identification is achieved by projecting the scaffold depths into a low-dimensional space using principal component analysis and subsequent Gaussian mixture clustering. Male and female whole genome sequences were used for this analysis.

- Using the method SexChrCov described in [99] with the 24-individual natural population.

- Using the method DifCover[100] which identifies regions in a reference genome for which the read coverage of one sample is significantly different from the read coverage of another sample when aligned to a common reference genome. The 24-individual natural population was used for this analysis.

- Using soap.coverage v2.7.9[101] to calculate the coverage (number of times each site was sequenced divided by the total number of sequenced sites) of each scaffold in each sample. For each scaffold, the male to female (M:F) fold change coverage was calculated as log2(average male coverage) – log2(average female coverage). The 24-individual natural population was used for this analysis.

F_{ST} and sex-biased heterozygosity. This approach has been previously used to find sex linked genomic regions in several studies[102,103]. Using the 24-individual natural population, F_{ST} was calculated using vcftools[95]. Sex-biased heterozygosity was defined as the log10 of the male heterozygosity:female heterozygosity, where heterozygosity is measured as the fraction of sites that are heterozygous. This ratio is expected to be zero for autosomal scaffolds and elevated on young sex scaffolds due to excess heterozygosity in males.

Identification of eventual female scaffolds that failed to map to the male reference genome. Vcftools and bedtools were used to extract female regions that did not map to the reference genome, consistently in the three re-sequenced female samples.

All candidate contigs were tested by PCR in 4 males and 4 females.

Synteny analyses, SDR evolutionary strata and transitions to co-sexuality

Whole-genome synteny comparisons were performed for each pair of chromosome-level assemblies using MCscan[104], both between different species, between sex chromosomes in the same species and between hermaphrodites and their closest relatives with U/V chromosomes. The putative gametologs between sex chromosomes that were predicted with MCscan were reassessed using OrthoFinder[105] and best reciprocal DIAMOND[106] hits.

We calculated the number of synonymous substitutions per synonymous site (*Ks*) for each pair of male and female gametologs as a proxy to assess the relative time at which both genes diverged from each other. The amino acid sequences of each pair of gametologs were aligned with MAFFT[107] and subsequently aligned into codons using pal2nal[108]. The *Ks* values were calculated using the model by Yang & Nielsen[109] as implemented in KaKs_calculator v2.0[110].

We evaluated the male or female identity of the genes in the co-sexual species whose orthologs were found within the SDR in their closest non-co-sexual relatives. For this, we compared the results obtained with MCscan[104] against the orthogroup prediction performed with OrthoFinder[105], with best reciprocal DIAMOND[106]

hits and by calculating gene trees for each orthogroup using an amino acid alignment with MAFFT[107] and gene tree reconstructions using FastTree[111].

Ancestral reconstruction of the male SDR

We searched for ortholog genes within the V-SDR of five species (*Ectocarpus* sp. 7, *Scytosiphon promiscuus*, *Undaria pinnatifida*, *Desmarestia herbacea* and *Dictyota dichotoma*) in our OrthoFinder results. Once we determined the evolutionary relationship of the genes within the V-SDR, we used the software Count[112] to estimate the ancestral content of the V-SDR throughout a phylogeny and determine the most likely scenario of V-SDR evolution in the brown algae. We employed posterior probabilities under a phylogenetic birth-and-death model with independent gain and loss rates across each branch in the phylogeny. We modeled the independent gain and loss rates through 10 gamma categories and performed 1000 optimization rounds with a convergence threshold on the likelihood > 0.1 to find the most fitting model for the data. The branch lengths in the tree that were used for the ancestral state reconstruction were retrieved from the molecular clock analysis performed by [14]. We distinguished between conserved V-SDR genes that are ancestral and parallel acquisitions of the same gene in the V-SDR by analyzing gene trees between male and female genomes, in addition to female transcriptome assemblies of *Dictyota dichotoma* and *Undaria pinnatifida*. Sequence alignments were done using MAFFT[107] with default settings and uploaded to http://www.phylogeny.fr/ platform. Alignments were further curated using Gblocks[113] (Min. seq. for flank pos.: 85%, Max. contig. nonconserved pos.: 8, Min. block length: 10). Trees were produced by PhyML[114] with default model and visualized in TreeDyn[115]. Approximate Likelihood-Ratio test (aLRT) was chosen as statistical test for branch support. We inferred the function of the ancestral V-SDR genes through the annotation of genes in *Ectocarpus* sp. 7 belonging to that orthogroup.

Genomic content across chromosomes

We used closely-related genome assemblies available in the PhaeoExplorer database (Deneoud et al, submitted) to assess the depletion of orthologs in the sex chromosome. We predicted one-to-one orthologs using OrthoFinder[105] between the following species pairs: *Ectocarpus* sp. 7 with *Ectocarpus siliculosus*, *Scytosiphon promiscuus* with *Chordaria linearis*, *Undaria pinnatifida* with *Saccharina japonica*, *Fucus serratus* with *Fucus distichus*, *Desmarestia herbacea* with *Desmarestia dudresnayi*, and *Dictyota dichotoma* with *Halopteris paniculata* (**Table S19**). We calculated the expected number of detectable orthologs for each chromosome and compared it against the observed number of detected orthologs using chi-squared tests. We performed Benjamini-Hochberg corrections to the *p*-values of the chi-squared tests to control the false discovery rate (FDR) in the analysis[116].

GenEra[30] was used by running DIAMOND in ultra-sensitive mode[106] against the NCBI NR database and all the PhaeoExplorer proteins (Deneoud et al, submitted) to perform a phylostratigraphic analysis (e-value threshold of 10^{-5}) and calculate the relative ages of each gene in each genome (**Table S20**). The gene age categories outside of the brown algae and *Schizocladia ischiensis* were based on the taxonomic classification of each species within the NCBI Taxonomy database[117], while the gene ages within the brown algae were manually assessed to reflect the evolutionary relationships obtained in the PhaeoExplorer maximum likelihood tree (Deneoud et al, submitted). We performed Wilcoxon rank-sum tests in R[118] to assess nonrandom differences in gene age distributions between pairs of chromosomes (**Table S11**). We performed Benjamini-

Hochberg corrections to the *p*-values of the Wilcoxon rank-sum tests to control the FDR in the analysis[116]. The gene ages responsible for these differences were found by evaluating the standardized residuals using mosaic plots (**Figs. S7-S13**). The relative gene ages in **Fig. 3B** and in **Figs. S7-S13** were plotted against the chromosome-level assemblies using karyoploteR[119].

We used the *Ks* values between pairs of species as a proxy for neutral mutation rates across six of the seven chromosome-level assemblies by using the most closely related genome assemblies available in the PhaeoExplorer database (Deneoud et al, submitted). We used the same set of one-to-one orthologs detected between species pairs as for the ortholog-depletion test (**Table S19**). However, the evolutionary distance between *Dictyota dichotoma* and *Halopteris paniculata* was so high that synonymous substitutions were already saturated, preventing us from calculating reliable *Ks* values for this species. The amino acid sequences of each pair of orthologs were aligned with MAFFT[107] and subsequently aligned into codons using pal2nal[108]. The *Ks* values were calculated using the model by Yang & Nielsen[109] as implemented in KaKs_calculator v2.0[110]. We also evaluated the difference in *Ks* values between the autosomes and the sex chromosomes through DFR-corrected Wilcoxon rank sum tests (**Table S13**). We calculated the protein-coding density, the density of transposable elements and the taxonomic identity of these transposable elements within 100 kb non-overlaping windows across each chromosome using bedtools[76] (**Table S21**). The differences in protein-coding space, TE content and TE classification between the autosomes and the sex chromosomes were also performed using DFR-corrected Wilcoxon rank sum tests (**Tables S7-S9**). All the genomic features were plotted using shinyCircos-V2.0[120].

Gene expression analysis

We used kallisto v.0.44.0[121] to calculate gene expression levels using 31-base-pair-long k-mers and 1000 bootstraps. Transcript abundances were then summed within genes using the tximport package[122] to obtain the expression level for each gene in TPM. Differential expression analysis was done in DESeq2 package[123] in R v.4.3.1, applying FC>=2 and Padj<0.05 cut-offs. Sex biased gene expression analysis in *Ectocarpus* sp. 7, *Scytosiphon promiscuus*, *Undaria pinnatifida*, *Desmarestia herbacea* and *Dictyota dichotoma* was estimated between mature male and female gametophytes (gametophytes baring reproductive structures). To discover genes with sporophyte biased expression in *Ectocarpus* sp.7, *Scytosiphon promiscuus*, *Undaria pinnatifida* and *Dictyota dichotoma* we first calculated the differential expression between male gametophytes and sporophytes, as well as female gametophytes and sporophytes. Genes that showed significant sporophyte-biased expression (FC>=2, padj<0.05) in both comparisons were considered sporophyte-biased.

A total of 314.2 M RNA-seq reads from *F. vesiculosus* male, female and vegetative tissue were assembled *de novo* with rnaSPAdes[124] using kmer values of 33 and 49. Assembly quality was assessed by (pseudo)mapping reads back onto the resulting assembly and retaining “good” contigs as defined using TransRate[125] with default settings. The resulting 159,108 contigs were aligned with BLASTx[72] against a database of Stramenopile proteins and those with top hits against brown algae (Phaeophyceae) were retained as the final curated reference transcriptome (36,394 contigs, N50 = 1770 bp). Transcript expression levels were determined by mapping the reads from all samples against the reference transcriptome using Bowtie2[126] and the RSEM-EBSeq[127] pipeline and relative expression values were recorded as transcripts per million (TPM). All samples used in the gene expression analysis can be found in **Table S22.**

REFERENCES

1. Bachtrog, D., Mank, J.E., Peichel, C.L., Kirkpatrick, M., Otto, S.P., Ashman, T.-L., Hahn, M.W., Kitano, J., Mayrose, I., Ming, R., et al. (2014). Sex Determination: Why So Many Ways of Doing It? PLoS Biol *12*, e1001899. 10.1371/journal.pbio.1001899.

2. Beukeboom, L.W., and Perrin, N. (2014). The Evolution of Sex Determination (Oxford University Press) 10.1093/acprof:oso/9780199657148.001.0001.

3. Vicoso, B. (2019). Molecular and evolutionary dynamics of animal sex-chromosome turnover. Nat Ecol Evol *3*, 1632–1641. 10.1038/s41559-019-1050-8.

4. Payseur, B.A., Presgraves, D.C., and Filatov, D.A. (2018). Introduction: Sex chromosomes and speciation. Mol Ecol *27*, 3745–3748. 10.1111/mec.14828.

5. Mignerot, L., Avia, K., Luthringer, R., Lipinska, A.P., Peters, A.F., Cock, J.M., and Coelho, S.M. (2019). A key role for sex chromosomes in the regulation of parthenogenesis in the brown alga Ectocarpus. PLoS Genet *15*, e1008211. 10.1371/journal.pgen.1008211.

6. Ma, W., and Rovatsos, M. (2022). Sex chromosome evolution: The remarkable diversity in the evolutionary rates and mechanisms. J Evol Biol *35*, 1581–1588. 10.1111/jeb.14119.

7. Umen, J., and Coelho, S. (2019). Algal Sex Determination and the Evolution of Anisogamy. Annu Rev Microbiol *73*, 267–291. 10.1146/annurev-micro-020518-120011.

8. Coelho, S.M., and Umen, J. (2021). Switching it up: algal insights into sexual transitions. Plant Reprod *34*, 287–296. 10.1007/s00497-021-00417-0.

9. Coelho, S.M., Mignerot, L., and Cock, J.M. (2019). Origin and evolution of sex-determination systems in the brown algae. New Phytologist *222*, 1751–1756. 10.1111/nph.15694.

10. Carey, S.B., Jenkins, J., Lovell, J.T., Maumus, F., Sreedasyam, A., Payton, A.C., Shu, S., Tiley, G.P., Fernandez-Pozo, N., Healey, A., et al. (2021). Gene-rich UV sex chromosomes harbor conserved regulators of sexual development. Sci Adv *7*. 10.1126/sciadv.abh2488.

11. Healey, A.L., Piatkowski, B., Lovell, J.T., Sreedasyam, A., Carey, S.B., Mamidi, S., Shu, S., Plott, C., Jenkins, J., Lawrence, T., et al. (2023). Newly identified sex chromosomes in the Sphagnum (peat moss) genome alter carbon sequestration and ecosystem dynamics. Nat Plants *9*, 238–254. 10.1038/s41477-022-01333-5.

12. Bowman, J.L., Kohchi, T., Yamato, K.T., Jenkins, J., Shu, S., Ishizaki, K., Yamaoka, S., Nishihama, R., Nakamura, Y., Berger, F., et al. (2017). Insights into Land Plant Evolution Garnered from the Marchantia polymorpha Genome. Cell *171*, 287-304.e15. 10.1016/j.cell.2017.09.030.

13. Silva, A.T., Gao, B., Fisher, K.M., Mishler, B.D., Ekwealor, J.T.B., Stark, L.R., Li, X., Zhang, D., Bowker, M.A., Brinda, J.C., et al. (2021). To dry perchance to live: Insights from the genome of the desiccation-tolerant biocrust moss *Syntrichia caninervis*. The Plant Journal *105*, 1339–1356. 10.1111/tpj.15116.

14. Heesch, S., Serrano-Serrano, M., Barrera-Redondo, J., Luthringer, R., Peters, A.F., Destombe, C., Cock, J.M., Valero, M., Roze, D., Salamin, N., et al. (2021). Evolution of life cycles and reproductive traits: Insights from the brown algae. J Evol Biol *34*, 992–1009. 10.1111/jeb.13880.

15. Bringloe, T.T., Starko, S., Wade, R.M., Vieira, C., Kawai, H., De Clerck, O., Cock, J.M., Coelho, S.M., Destombe, C., Valero, M., et al. (2020). Phylogeny and Evolution of the Brown Algae. CRC Crit Rev Plant Sci *39*, 281–321. 10.1080/07352689.2020.1787679.

16. Kawai, H., Maeba, S., Sasaki, H., Okuda, K., and Henry, E.C. (2003). Schizocladis ischiensis: A new filamentous marine chromophyte belonging to a new class, Schizocladiophyceae. Protist *154*, 211–228. 10.1078/143446103322166518.

17. Kawai, H., Hanyuda, T., Draisma, S.G.A., Wilce, R.T., and Andersen, R.A. (2015). Molecular phylogeny of two unusual brown algae, *Phaeostrophion irregulare* and *Platysiphon glacialis* , proposal of the Stschapoviales ord. nov. and Platysiphonaceae fam. nov., and a re-examination of divergence times for brown algal orders. J Phycol *51*, 918–928. 10.1111/jpy.12332.

18. Simakov, O., Bredeson, J., Berkoff, K., Marletaz, F., Mitros, T., Schultz, D.T., O'Connell, B.L., Dear, P., Martinez, D.E., Steele, R.E., et al. (2022). Deeply conserved synteny and the evolution of metazoan chromosomes. Sci Adv *8*. 10.1126/sciadv.abi5884.

19. Zhou, Y., Zhan, X., Jin, J., Zhou, L., Bergman, J., Li, X., Rousselle, M.M.C., Belles, M.R., Zhao, L., Fang, M., et al. (2023). Eighty million years of rapid evolution of the primate Y chromosome. Nat Ecol Evol *7*, 1114–1130. 10.1038/s41559-022-01974-x.

20. Ahmed, S., Cock, J.M., Pessia, E., Luthringer, R., Cormier, A., Robuchon, M., Sterck, L., Peters, A.F., Dittami, S.M., Corre, E., et al. (2014). A Haploid System of Sex Determination in the Brown Alga Ectocarpus sp. Current Biology *24*, 1945–1957. 10.1016/j.cub.2014.07.042.

21. Lipinska, A.P., Toda, N.R.T., Heesch, S., Peters, A.F., Cock, J.M., and Coelho, S.M. (2017). Multiple gene movements into and out of haploid sex chromosomes. Genome Biol *18*, 104. 10.1186/s13059-017-1201-7.

22. Bull, J.J. (1978). Sex Chromosomes in Haploid Dioecy: A Unique Contrast to Muller's Theory for Diploid Dioecy. Am Nat *112*, 245–250. 10.1086/283267.

23. Charlesworth, D. (2015). Plant contributions to our understanding of sex chromosome evolution. New Phytologist *208*, 52–65. 10.1111/nph.13497.

24. Bolwell, G.P., Callow, J.A., Callow, M.E., and Evans, L. V. (1979). Fertilization in brown algae: II. evidence for lectin-sensitive complementary receptors involved in gamete recognition in *Fucus serratus*. J Cell Sci *36*, 19–30. 10.1242/jcs.36.1.19.

25. Zhao, Z.-S., Leung, T., Manser, E., and Lim, L. (1995). Pheromone Signalling in *Saccharomyces cerevisiae* Requires the Small GTP-Binding Protein Cdc42p and Its Activator *CDC24*. Mol Cell Biol *15*, 5246–5257. 10.1128/MCB.15.10.5246.

26. Cossard, G.G., Godfroy, O., Nehr, Z., Cruaud, C., Cock, J.M., Lipinska, A.P., and Coelho, S.M. (2022). Selection drives convergent gene expression changes during transitions to co-sexuality in haploid sexual systems. Nat Ecol Evol *6*, 579–589. 10.1038/s41559-022-01692-4.

27. Johnson, N.A., and Lachance, J. (2012). The genetics of sex chromosomes: evolution and implications for hybrid incompatibility. Ann N Y Acad Sci *1256*, E1–E22. 10.1111/j.1749-6632.2012.06748.x.

28. Luthringer, R., Lipinska, A.P., Roze, D., Cormier, A., Macaisne, N., Peters, A.F., Cock, J.M., and Coelho, S.M. (2015). The Pseudoautosomal Regions of the U/V Sex Chromosomes of the Brown Alga *Ectocarpus* Exhibit Unusual Features. Mol Biol Evol *32*, 2973–2985. 10.1093/molbev/msv173.

29. Domazet-Lošo, T., Brajković, J., and Tautz, D. (2007). A phylostratigraphy approach to uncover the genomic history of major adaptations in metazoan lineages. Trends in Genetics *23*, 533–539. 10.1016/j.tig.2007.08.014.

30. Barrera-Redondo, J., Lotharukpong, J.S., Drost, H.-G., and Coelho, S.M. (2023). Uncovering gene-family founder events during major evolutionary transitions in animals, plants and fungi using GenEra. Genome Biol *24*, 54. 10.1186/s13059-023-02895-z.

31. Van Oss, S.B., and Carvunis, A.-R. (2019). De novo gene birth. PLoS Genet *15*, e1008160. 10.1371/journal.pgen.1008160.

32. Tautz, D., and Domazet-Lošo, T. (2011). The evolutionary origin of orphan genes. Nat Rev Genet *12*, 692–702. 10.1038/nrg3053.

33. Weisman, C.M., Murray, A.W., and Eddy, S.R. (2020). Many, but not all, lineage-specific genes can be explained by homology detection failure. PLoS Biol *18*, e3000862. 10.1371/journal.pbio.3000862.

34. Kimura, M. (1977). Preponderance of synonymous changes as evidence for the neutral theory of molecular evolution. Nature *267*, 275–276. 10.1038/267275a0.

35. King, J.L., and Jukes, T.H. (1969). Non-Darwinian Evolution. Science (1979) *164*, 788–798. 10.1126/science.164.3881.788.

36. Eyre-Walker, A., and Keightley, P.D. (1999). High genomic deleterious mutation rates in hominids. Nature *397*, 344–347. 10.1038/16915.

37. Keightley, P.D., and Eyre-Walker, A. (2000). Deleterious Mutations and the Evolution of Sex. Science (1979) *290*, 331–333. 10.1126/science.290.5490.331.

38. Hatchett, W.J., Jueterbock, A.O., Kopp, M., Coyer, J.A., Coelho, S.M., Hoarau, G., and Lipinska, A.P. (2023). Evolutionary dynamics of sex-biased gene expression in a young <scp>XY</scp> system: insights from the brown alga genus *Fucus*. New Phytologist *238*, 422–437. 10.1111/nph.18710.

39. Clayton, M.N. (1987). Isogamy and a Fucalean type of life history in the Antarctic brown alga *Ascoseira mirabilis* (Ascoseirales, Phaeophyta). Botanica Marina *30*, 447–454. 10.1515/botm.1987.30.6.447.

40. Cánovas, F.G., Mota, C.F., Serrão, E.A., and Pearson, G.A. (2011). Driving south: a multi-gene phylogeny of the brown algal family Fucaceae reveals relationships and recent drivers of a marine radiation. BMC Evol Biol *11*, 371. 10.1186/1471-2148-11-371.

41. Crossman, A., and Charlesworth, D. (2014). Breakdown of dioecy: models where males acquire cosexual functions. Evolution (N Y) *68*, 426–440. 10.1111/evo.12283.

42. Lv, J., Havlak, P., and Putnam, N.H. (2011). Constraints on genes shape long-term conservation of macro-synteny in metazoan genomes. BMC Bioinformatics *12*, S11. 10.1186/1471-2105-12-S9-S11.

43. Irimia, M., Tena, J.J., Alexis, M.S., Fernandez-Miñan, A., Maeso, I., Bogdanović, O., de la Calle-Mustienes, E., Roy, S.W., Gómez-Skarmeta, J.L., and Fraser, H.B. (2012). Extensive conservation of ancient microsynteny across metazoans due to *cis* -regulatory constraints. Genome Res *22*, 2356–2367. 10.1101/gr.139725.112.

44. Gray, Y.H.M. (2000). It takes two transposons to tango:transposable-element-mediated chromosomal rearrangements. Trends in Genetics *16*, 461–468. 10.1016/S0168-9525(00)02104-1.

45. Lee, S.C., Ni, M., Li, W., Shertz, C., and Heitman, J. (2010). The Evolution of Sex: a Perspective from the Fungal Kingdom. Microbiology and Molecular Biology Reviews *74*, 298–340. 10.1128/MMBR.00005-10.

46. Duhamel, M., Hood, M.E., Rodríguez de la Vega, R.C., and Giraud, T. (2023). Dynamics of transposable element accumulation in the non-recombining regions of mating-type chromosomes in anther-smut fungi. Nat Commun *14*, 5692. 10.1038/s41467-023-41413-4.

47. Dolgin, E.S., and Charlesworth, B. (2008). The Effects of Recombination Rate on the Distribution and Abundance of Transposable Elements. Genetics *178*, 2169–2177. 10.1534/genetics.107.082743.

48. Charlesworth, D. (2017). Evolution of recombination rates between sex chromosomes. Philosophical Transactions of the Royal Society B: Biological Sciences *372*, 20160456. 10.1098/rstb.2016.0456.

49. Jordan, C.Y., and Charlesworth, D. (2012). The potential for sexually antagonistic polymorphism in different genome regions. Evolution (N Y) *66*, 505–516. 10.1111/j.1558-5646.2011.01448.x.

50. Jeffries, D.L., Gerchen, J.F., Scharmann, M., and Pannell, J.R. (2021). A neutral model for the loss of recombination on sex chromosomes. Philosophical Transactions of the Royal Society B: Biological Sciences *376*, 20200096. 10.1098/rstb.2020.0096.

51. Olito, C., and Abbott, J.K. (2023). The evolution of suppressed recombination between sex chromosomes and the lengths of evolutionary strata. Evolution (N Y) *77*, 1077–1090. 10.1093/evolut/qpad023.

52. Jay, P., Tezenas, E., Véber, A., and Giraud, T. (2022). Sheltering of deleterious mutations explains the stepwise extension of recombination suppression on sex chromosomes and other supergenes. PLoS Biol *20*, e3001698. 10.1371/journal.pbio.3001698.

53. Lenormand, T., and Roze, D. (2022). Y recombination arrest and degeneration in the absence of sexual dimorphism. Science (1979) *375*, 663–666. 10.1126/science.abj1813.

54. Cox, R.M., and Calsbeek, R. (2009). Sexually Antagonistic Selection, Sexual Dimorphism, and the Resolution of Intralocus Sexual Conflict. Am Nat *173*, 176–187. 10.1086/595841.

55. Scharmann, M., Rebelo, A.G., and Pannell, J.R. (2021). High rates of evolution preceded shifts to sex-biased gene expression in Leucadendron, the most sexually dimorphic angiosperms. Elife *10*. 10.7554/eLife.67485.

56. Charlesworth, B. (1978). Model for evolution of Y chromosomes and dosage compensation. Proceedings of the National Academy of Sciences *75*, 5618–5622. 10.1073/pnas.75.11.5618.

57. Lenormand, T., Fyon, F., Sun, E., and Roze, D. (2020). Sex Chromosome Degeneration by Regulatory Evolution. Current Biology *30*, 3001-3006.e5. 10.1016/j.cub.2020.05.052.

58. Coelho, S.M., Gueno, J., Lipinska, A.P., Cock, J.M., and Umen, J.G. (2018). UV Chromosomes and Haploid Sexual Systems. Trends Plant Sci *23*, 794–807. 10.1016/j.tplants.2018.06.005.

59. Charlesworth, D. (2022). The mysterious sex chromosomes of haploid plants. Heredity (Edinb) *129*, 17–21. 10.1038/s41437-022-00524-2.

60. Ivics, Z., and Izsvák, Z. (2010). The expanding universe of transposon technologies for gene and cell engineering. Mob DNA *1*, 25. 10.1186/1759-8753-1-25.

61. Gueno, J., Borg, M., Bourdareau, S., Cossard, G., Godfroy, O., Lipinska, A., Tirichine, L., Cock, J.M., and Coelho, S.M. (2022). Chromatin landscape associated with sexual differentiation in a UV sex determination system. Nucleic Acids Res *50*, 3307–3322. 10.1093/nar/gkac145.

62. Makova, K.D., and Hardison, R.C. (2015). The effects of chromatin organization on variation in mutation rates in the genome. Nat Rev Genet *16*, 213–223. 10.1038/nrg3890.

63. Cortez, D., Marin, R., Toledo-Flores, D., Froidevaux, L., Liechti, A., Waters, P.D., Grützner, F., and Kaessmann, H. (2014). Origins and functional evolution of Y chromosomes across mammals. Nature *508*, 488–493. 10.1038/nature13151.

64. Herpin, A., and Schartl, M. (2015). Plasticity of gene-regulatory networks controlling sex determination: of masters, slaves, usual suspects, newcomers, and usurpators. EMBO Rep *16*, 1260–1274. 10.15252/embr.201540667.

65. Assis, R., Zhou, Q., and Bachtrog, D. (2012). Sex-Biased Transcriptome Evolution in Drosophila. Genome Biol Evol *4*, 1189–1200. 10.1093/gbe/evs093.

66. Vigneau, J., Martinho, C., Godfroy, O., Zheng, M., Haas, F.B., Borg, M., and Coelho, S.M. (2023). Sex chromosome dominance in a UV sexual system. bioRxiv, 1–31.

67. Starr, R.C., and Zeikus, J.A. (1993). UTEX-THE CULTURE COLLECTION OF ALGAE AT THE UNIVERSITY OF TEXAS AT AUSTIN 1993 LIST OF CULTURES1. J Phycol *29*, 1–106. 10.1111/j.0022-3646.1993.00001.x.

68. Cormier, A., Avia, K., Sterck, L., Derrien, T., Wucher, V., Andres, G., Monsoor, M., Godfroy, O., Lipinska, A., Perrineau, M., et al. (2017). Re-annotation, improved large-scale assembly and establishment of a catalogue of noncoding loci for the genome of the model brown alga *Ectocarpus*. New Phytologist *214*, 219–232. 10.1111/nph.14321.

69. Shan, T., Yuan, J., Su, L., Li, J., Leng, X., Zhang, Y., Gao, H., and Pang, S. (2020). First Genome of the Brown Alga Undaria pinnatifida: Chromosome-Level Assembly Using PacBio and Hi-C Technologies. Front Genet *11*. 10.3389/fgene.2020.00140.

70. Wick, R.R., Judd, L.M., and Holt, K.E. (2019). Performance of neural network basecalling tools for Oxford Nanopore sequencing. Genome Biol *20*, 129. 10.1186/s13059-019-1727-y.

71. Wood, D.E., Lu, J., and Langmead, B. (2019). Improved metagenomic analysis with Kraken 2. Genome Biol *20*, 257. 10.1186/s13059-019-1891-0.

72. Altschul, S.F., Gish, W., Miller, W., Myers, E.W., and Lipman, D.J. (1990). Basic local alignment search tool. J Mol Biol *215*, 403–410. 10.1016/S0022-2836(05)80360-2.

73. Huson, D.H., Auch, A.F., Qi, J., and Schuster, S.C. (2007). MEGAN analysis of metagenomic data. Genome Res *17*, 377–386. 10.1101/gr.5969107.

74. Kolmogorov, M., Yuan, J., Lin, Y., and Pevzner, P.A. (2019). Assembly of long, error-prone reads using repeat graphs. Nat Biotechnol *37*, 540–546. 10.1038/s41587-019-0072-8.

75. Price, A.L., Jones, N.C., and Pevzner, P.A. (2005). De novo identification of repeat families in large genomes. Bioinformatics *21*, i351–i358. 10.1093/bioinformatics/bti1018.

76. Quinlan, A.R., and Hall, I.M. (2010). BEDTools: a flexible suite of utilities for comparing genomic features. Bioinformatics *26*, 841–842. 10.1093/bioinformatics/btq033.

77. Dobin, A., Davis, C.A., Schlesinger, F., Drenkow, J., Zaleski, C., Jha, S., Batut, P., Chaisson, M., and Gingeras, T.R. (2013). STAR: ultrafast universal RNA-seq aligner. Bioinformatics *29*, 15–21. 10.1093/bioinformatics/bts635.

78. Hoff, K.J., Lange, S., Lomsadze, A., Borodovsky, M., and Stanke, M. (2016). BRAKER1: Unsupervised RNA-Seq-Based Genome Annotation with GeneMark-ET and AUGUSTUS. Bioinformatics *32*, 767–769. 10.1093/bioinformatics/btv661.

79. Bolger, A.M., Lohse, M., and Usadel, B. (2014). Trimmomatic: a flexible trimmer for Illumina sequence data. Bioinformatics *30*, 2114–2120. 10.1093/bioinformatics/btu170.

80. Li, H. (2013). Aligning sequence reads, clone sequences and assembly contigs with BWA-MEM. arXiv preprint arXiv *00*, 3. arXiv:1303.3997 [q-bio.GN].

81. Durand, N.C., Shamim, M.S., Machol, I., Rao, S.S.P., Huntley, M.H., Lander, E.S., and Aiden, E.L. (2016). Juicer Provides a One-Click System for Analyzing Loop-Resolution Hi-C Experiments. Cell Syst *3*, 95–98. 10.1016/j.cels.2016.07.002.

82. Dudchenko, O., Batra, S.S., Omer, A.D., Nyquist, S.K., Hoeger, M., Durand, N.C., Shamim, M.S., Machol, I., Lander, E.S., Aiden, A.P., et al. (2017). De novo assembly of the *Aedes aegypti* genome using Hi-C yields chromosome-length scaffolds. Science (1979) *356*, 92–95. 10.1126/science.aal3327.

83. Durand, N.C., Robinson, J.T., Shamim, M.S., Machol, I., Mesirov, J.P., Lander, E.S., and Aiden, E.L. (2016). Juicebox Provides a Visualization System for Hi-C Contact Maps with Unlimited Zoom. Cell Syst *3*, 99–101. 10.1016/j.cels.2015.07.012.

84. Shumate, A., and Salzberg, S.L. (2021). Liftoff: accurate mapping of gene annotations. Bioinformatics *37*, 1639–1643. 10.1093/bioinformatics/btaa1016.

85. Flynn, J.M., Hubley, R., Goubert, C., Rosen, J., Clark, A.G., Feschotte, C., and Smit, A.F. (2020). RepeatModeler2 for automated genomic discovery of transposable element families. Proceedings of the National Academy of Sciences *117*, 9451–9457. 10.1073/pnas.1921046117.

86. Alonge, M., Lebeigle, L., Kirsche, M., Jenike, K., Ou, S., Aganezov, S., Wang, X., Lippman, Z.B., Schatz, M.C., and Soyk, S. (2022). Automated assembly scaffolding using RagTag elevates a new tomato system for high-throughput genome editing. Genome Biol *23*, 258. 10.1186/s13059-022-02823-7.

87. Carvalho, A.B., and Clark, A.G. (2013). Efficient identification of Y chromosome sequences in the human and *Drosophila* genomes. Genome Res *23*, 1894–1907. 10.1101/gr.156034.113.

88. Vicoso, B., Emerson, J.J., Zektser, Y., Mahajan, S., and Bachtrog, D. (2013). Comparative Sex Chromosome Genomics in Snakes: Differentiation, Evolutionary Strata, and Lack of Global Dosage Compensation. PLoS Biol *11*, e1001643. 10.1371/journal.pbio.1001643.

89. Marçais, G., and Kingsford, C. (2011). A fast, lock-free approach for efficient parallel counting of occurrences of *k* -mers. Bioinformatics *27*, 764–770. 10.1093/bioinformatics/btr011.

90. Shen, W., Le, S., Li, Y., and Hu, F. (2016). SeqKit: A Cross-Platform and Ultrafast Toolkit for FASTA/Q File Manipulation. PLoS One *11*, e0163962. 10.1371/journal.pone.0163962.

91. Kim, D., Paggi, J.M., Park, C., Bennett, C., and Salzberg, S.L. (2019). Graph-based genome alignment and genotyping with HISAT2 and HISAT-genotype. Nat Biotechnol *37*, 907–915. 10.1038/s41587-019-0201-4.

92. Pedersen, B.S., and Quinlan, A.R. (2018). Mosdepth: quick coverage calculation for genomes and exomes. Bioinformatics *34*, 867–868. 10.1093/bioinformatics/btx699.

93. Avia, K., Coelho, S.M., Montecinos, G.J., Cormier, A., Lerck, F., Mauger, S., Faugeron, S., Valero, M., Cock, J.M., and Boudry, P. (2017). High-density genetic map and identification of QTLs for responses to temperature and salinity stresses in the model brown alga Ectocarpus. Sci Rep *7*, 43241. 10.1038/srep43241.

94. Rochette, N.C., Rivera-Colón, A.G., and Catchen, J.M. (2019). Stacks 2: Analytical methods for paired-end sequencing improve RADseq-based population genomics. Mol Ecol *28*, 4737–4754. 10.1111/mec.15253.

95. Danecek, P., Auton, A., Abecasis, G., Albers, C.A., Banks, E., DePristo, M.A., Handsaker, R.E., Lunter, G., Marth, G.T., Sherry, S.T., et al. (2011). The variant call format and VCFtools. Bioinformatics *27*, 2156–2158. 10.1093/bioinformatics/btr330.

96. Li, H., Handsaker, B., Wysoker, A., Fennell, T., Ruan, J., Homer, N., Marth, G., Abecasis, G., and Durbin, R. (2009). The Sequence Alignment/Map format and SAMtools. Bioinformatics *25*, 2078–2079. 10.1093/bioinformatics/btp352.

97. Rastas, P. (2017). Lep-MAP3: robust linkage mapping even for low-coverage whole genome sequencing data. Bioinformatics *33*, 3726–3732. 10.1093/bioinformatics/btx494.

98. Nursyifa, C., Brüniche-Olsen, A., Garcia-Erill, G., Heller, R., and Albrechtsen, A. (2022). Joint identification of sex and sex-linked scaffolds in non-model organisms using low depth sequencing data. Mol Ecol Resour *22*, 458–467. 10.1111/1755-0998.13491.

99. Malde, K., Skern, R., and Glover, K.A. (2019). Using sequencing coverage statistics to identify sex chromosomes in minke whales. ArXiv, 1902.06654.

100. Smith, J.J., Timoshevskaya, N., Ye, C., Holt, C., Keinath, M.C., Parker, H.J., Cook, M.E., Hess, J.E., Narum, S.R., Lamanna, F., et al. (2018). The sea lamprey germline genome provides insights into programmed genome rearrangement and vertebrate evolution. Nat Genet *50*, 270–277. 10.1038/s41588-017-0036-1.

101. Darolti, I., Wright, A.E., Sandkam, B.A., Morris, J., Bloch, N.I., Farré, M., Fuller, R.C., Bourne, G.R., Larkin, D.M., Breden, F., et al. (2019). Extreme heterogeneity in sex chromosome differentiation and dosage compensation in livebearers. Proceedings of the National Academy of Sciences *116*, 19031–19036. 10.1073/pnas.1905298116.

102. Brelsford, A., Lavanchy, G., Sermier, R., Rausch, A., and Perrin, N. (2017). Identifying homomorphic sex chromosomes from wild-caught adults with limited genomic resources. Mol Ecol Resour *17*, 752–759. 10.1111/1755-0998.12624.

103. Toups, M.A., Rodrigues, N., Perrin, N., and Kirkpatrick, M. (2019). A reciprocal translocation radically reshapes sex-linked inheritance in the common frog. Mol Ecol *28*, 1877–1889. 10.1111/mec.14990.

104. Tang, H., Bowers, J.E., Wang, X., Ming, R., Alam, M., and Paterson, A.H. (2008). Synteny and Collinearity in Plant Genomes. Science (1979) *320*, 486–488. 10.1126/science.1153917.

105. Emms, D.M., and Kelly, S. (2019). OrthoFinder: phylogenetic orthology inference for comparative genomics. Genome Biol *20*, 238. 10.1186/s13059-019-1832-y.

106. Buchfink, B., Reuter, K., and Drost, H.-G. (2021). Sensitive protein alignments at tree-of-life scale using DIAMOND. Nat Methods *18*, 366–368. 10.1038/s41592-021-01101-x.

107. Katoh, K., Misawa, K., Kuma, K., and Miyata, T. (2002). MAFFT: a novel method for rapid multiple sequence alignment based on fast Fourier transform. Nucleic Acids Res *30*, 3059–3066. 10.1093/nar/gkf436.

108. Suyama, M., Torrents, D., and Bork, P. (2006). PAL2NAL: Robust conversion of protein sequence alignments into the corresponding codon alignments. Nucleic Acids Res *34*, 609–612. 10.1093/nar/gkl315.

109. Yang, Z., and Nielsen, R. (2000). Estimating Synonymous and Nonsynonymous Substitution Rates Under Realistic Evolutionary Models. Mol Biol Evol *17*, 32–43. 10.1093/oxfordjournals.molbev.a026236.

110. Wang, D., Zhang, Y., Zhang, Z., Zhu, J., and Yu, J. (2010). KaKs_Calculator 2.0: A Toolkit Incorporating Gamma-Series Methods and Sliding Window Strategies. Genomics Proteomics Bioinformatics *8*, 77–80. 10.1016/S1672-0229(10)60008-3.

111. Price, M.N., Dehal, P.S., and Arkin, A.P. (2009). Fasttree: Computing large minimum evolution trees with profiles instead of a distance matrix. Mol Biol Evol *26*, 1641–1650. 10.1093/molbev/msp077.

112. Csűös, M. (2010). Count: evolutionary analysis of phylogenetic profiles with parsimony and likelihood. Bioinformatics *26*, 1910–1912. 10.1093/bioinformatics/btq315.

113. Castresana, J. (2000). Selection of Conserved Blocks from Multiple Alignments for Their Use in Phylogenetic Analysis. Mol Biol Evol *17*, 540–552. 10.1093/oxfordjournals.molbev.a026334.

114. Guindon, S., Dufayard, J.F., Lefort, V., Anisimova, M., Hordijk, W., and Gascuel, O. (2010). New Algorithms and Methods to Estimate Maximum-Likelihood Phylogenies: Assessing the Performance of PhyML 3.0. Syst Biol *59*, 307–321. 10.1093/sysbio/syq010.

115. Chevenet, F., Brun, C., Bañuls, A.-L., Jacq, B., and Christen, R. (2006). TreeDyn: towards dynamic graphics and annotations for analyses of trees. BMC Bioinformatics *7*, 439. 10.1186/1471-2105-7-439.

116. Benjamini, Y., and Hochberg, Y. (1995). Controlling the False Discovery Rate: A Practical and Powerful Approach to Multiple Testing. Journal of the Royal Statistical Society *57*, 289–300. 10.2307/2346101.

117. Schoch, C.L., Ciufo, S., Domrachev, M., Hotton, C.L., Kannan, S., Khovanskaya, R., Leipe, D., Mcveigh, R., O'Neill, K., Robbertse, B., et al. (2020). NCBI Taxonomy: a comprehensive update on curation, resources and tools. Database *2020*. 10.1093/database/baaa062.

118. Team, R.C. (2021). R: A language and environment for statistical computing. Preprint at R Foundation for Statistical Computing.

119. Gel, B., and Serra, E. (2017). karyoploteR: an R/Bioconductor package to plot customizable genomes displaying arbitrary data. Bioinformatics *33*, 3088–3090. 10.1093/bioinformatics/btx346.

120. Wang, Y., Jia, L., Tian, G., Dong, Y., Zhang, X., Zhou, Z., Luo, X., Li, Y., and Yao, W. (2023). shinyCircos-V2.0: Leveraging the creation of Circos plot with enhanced usability and advanced features. iMeta *2*. 10.1002/imt2.109.

121. Bray, N.L., Pimentel, H., Melsted, P., and Pachter, L. (2016). Near-optimal probabilistic RNA-seq quantification. Nat Biotechnol *34*, 525–527. 10.1038/nbt.3519.

122. Soneson, C., Love, M.I., and Robinson, M.D. (2015). Differential analyses for RNA-seq: transcript-level estimates improve gene-level inferences. F1000Res *4*, 1521. 10.12688/f1000research.7563.1.

123. Love, M.I., Huber, W., and Anders, S. (2014). Moderated estimation of fold change and dispersion for RNA-seq data with DESeq2. Genome Biol *15*, 550. 10.1186/s13059-014-0550-8.

124. Bushmanova, E., Antipov, D., Lapidus, A., and Prjibelski, A.D. (2019). rnaSPAdes: a de novo transcriptome assembler and its application to RNA-Seq data. Gigascience *8*. 10.1093/gigascience/giz100.

125. Smith-Unna, R., Boursnell, C., Patro, R., Hibberd, J.M., and Kelly, S. (2016). TransRate: reference-free quality assessment of de novo transcriptome assemblies. Genome Res *26*, 1134–1144. 10.1101/gr.196469.115.

126. Langmead, B., and Salzberg, S.L. (2012). Fast gapped-read alignment with Bowtie 2. Nat Methods *9*, 357–359. 10.1038/nmeth.1923.

127. Leng, N., Dawson, J.A., Thomson, J.A., Ruotti, V., Rissman, A.I., Smits, B.M.G., Haag, J.D., Gould, M.N., Stewart, R.M., and Kendziorski, C. (2013). EBSeq: an empirical Bayes hierarchical model for inference in RNA-seq experiments. Bioinformatics *29*, 1035–1043. 10.1093/bioinformatics/btt087.